Mathematical Medicine and Biology (2011) **28**, 47−84
doi:10.1093/imammb/dqq005
Advance Access publication on May 3, 2010

Grow with the flow: a spatial–temporal model of platelet deposition and blood coagulation under flow

KARIN LEIDERMAN*
Department of Mathematics, University of Utah, 155 South 1400 East, Room 233, Salt Lake City, UT 84112-0090, USA
*Corresponding author: karin@math.utah.edu

AND

AARON L. FOGELSON
Departments of Mathematics and Bioengineering, University of Utah, 155 South 1400 East, Room 233, Salt Lake City, UT 84112-0090, USA
fogelson@math.utah.edu

[Received on 10 November 2009; revised on 15 February 2010; accepted on 30 March 2010]

The body's response to vascular injury involves two intertwined processes: platelet aggregation and coagulation. Platelet aggregation is a predominantly physical process, whereby platelets clump together, and coagulation is a cascade of biochemical enzyme reactions. Thrombin, the major product of coagulation, directly couples the biochemical system to platelet aggregation by activating platelets and by cleaving fibrinogen into fibrin monomers that polymerize to form a mesh that stabilizes platelet aggregates. Together, the fibrin mesh and the platelet aggregates comprise a thrombus that can grow to occlusive diameters. Transport of coagulation proteins and platelets to and from an injury is controlled largely by the dynamics of the blood flow. To explore how blood flow affects the growth of thrombi and how the growing masses, in turn, feed back and affect the flow, we have developed the first spatial–temporal mathematical model of platelet aggregation and blood coagulation under flow that includes detailed descriptions of coagulation biochemistry, chemical activation and deposition of blood platelets, as well as the two-way interaction between the fluid dynamics and the growing platelet mass. We present this model and use it to explain what underlies the threshold behaviour of the coagulation system's production of thrombin and to show how wall shear rate and near-wall enhanced platelet concentrations affect the development of growing thrombi. By accounting for the porous nature of the thrombus, we also demonstrate how advective and diffusive transport to and within the thrombus affects its growth at different stages and spatial locations.

Keywords: thrombosis; mathematical model.

1. Introduction

In this paper, we present a spatial–temporal mathematical model of the processes that occur when a blood clot (thrombus) forms inside of a blood vessel. These processes are responsible for normal 'hemostasis', which maintains the integrity of the vasculature and are implicated in its pathological counterpart 'thrombosis', which underlies most heart attacks and strokes. The 'clotting response' is comprised of complex and diverse biochemical, biophysical and biomechanical interactions. Because of its extreme medical importance, the component pieces of this process have been and continue to be subjects of intense laboratory research. The sheer complexity of the disparate dynamic interactions that

make up the clotting response as well as the fact that multiple temporal and spatial scales are important in the processes make it very difficult, using traditional experimental approaches alone, to piece together a quantitative picture of how the system as a whole functions. The mathematical modelling we present is aimed at integrating together the knowledge obtained from laboratory experimentation to develop a quantitative understanding of how the many pieces of the clotting system function together and, ultimately, to develop the ability to make accurate quantitative predictions of this behaviour.

Injury to the endothelial cell lining of a blood vessel triggers the intertwined processes of platelet deposition and coagulation. The former starts with platelet adhesion to the exposed subendothelium, which causes these should be "platelets" to become activated and to secrete platelet-activating chemicals into the plasma. These chemicals may activate platelets in the blood (without their contacting the subendothelium directly) making them able to cohere to one another and to the already wall-adherent platelets. The mass that results is called a platelet thrombus or platelet plug. Coagulation starts with enzyme reactions on the exposed subendothelium and progresses with other enzyme reactions on the surfaces of activated platelets. A major product of the coagulation reaction network is the critical enzyme thrombin which (i) affects earlier reaction steps to speed its own production, (ii) activates platelets and (iii) acts on the soluble plasma protein fibrinogen to produce insoluble fibrin monomers, which spontaneously polymerize in a process that ultimately leads to a fibrin protein gel within and surrounding the platelet thrombus.

A schematic of these processes is given in Fig. 1, and a detailed discussion of the reactions and interactions can be found in Kuharsky & Fogelson (2001). Excellent reviews can be found in Hemker &

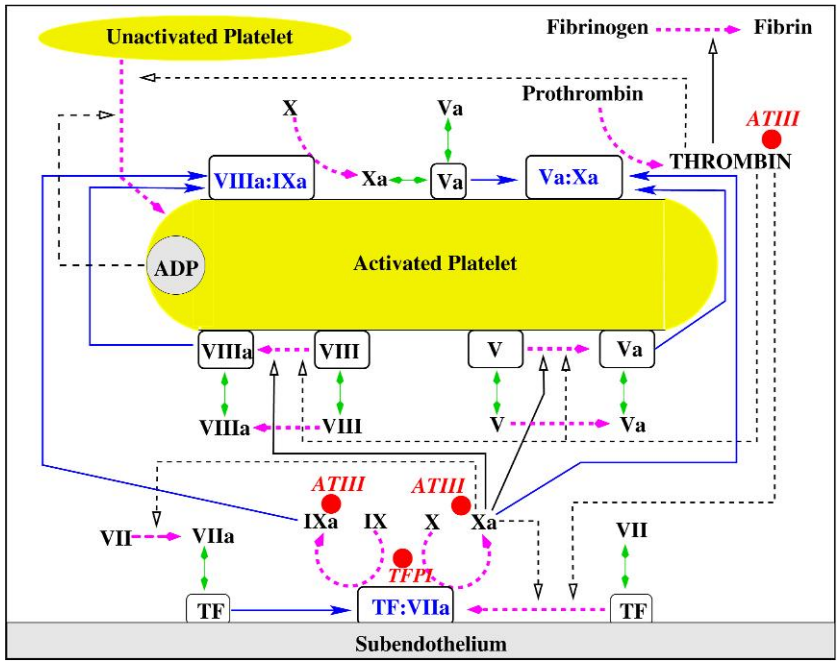

FIG. 1. Schematic of coagulation reactions. Dashed magenta arrows show cellular or chemical activation processes. Blue arrows indicate chemical transport in the fluid or on a surface. Green segments with two arrowheads depict binding and unbinding from a surface. Rectangular boxes indicate surface-bound species. Solid black lines with open arrows show enzyme action in a forward direction, while dashed black lines with open arrows show feedback action of enzymes. Red disks indicate chemical inhibitors.

Kessels (1991), Jesty & Nemerson (1995) and Mann *et al*. (1990). Here, we outline the salient features of the coagulation and platelet deposition processes while using the following abbreviations: TF, tissue factor; APC, activated protein C; TFPI, tissue factor pathway inhibitor; ADP, adenosine diphosphate; ATIII, antithrombin-III.

- Each of the coagulation proteins has an inactive and an active form. The inactive zymogens are factors VII, IX, X, and II (prothrombin) and have corresponding active enzymes factors VIIa, IXa, Xa, and IIa (thrombin), respectively. The inactive/active cofactor pairs are factors V and Va, and factors VIII and VIIIa.
- Three enzyme complexes play major parts in coagulation, the tissue factor complex on the subendothelium (TF:VIIa) and the tenase (VIIIa:IXa) and prothrombinase (Va:Xa) complexes on the surface of activated platelets. In these complexes, a cofactor TF, VIIIa or Va helps tremendously to increase the catalytic effectiveness of the corresponding enzyme (VIIa, IXa and Xa, respectively) compared to that of the same enzyme molecule without its cofactor.
- The reactions are initiated when VIIa binds to TF molecules exposed to the blood by the injury. The complex TF:VIIa activates zymogens IX and X to enzymes IXa and Xa, respectively. Each of these enzymes can become part of an enzyme complex on the surface of an activated platelet. For these complexes to form, there must be activated platelets nearby, the enzymes must make their way through the fluid from the subendothelial surface to the surface of one of the activated platelets and the active cofactor molecules, VIIIa and Va, must be available and bound to that activated platelet's surface. Early in the process, platelet-bound Xa activates the cofactors VIIIa and Va on the platelet surface.
- When a tenase (VIIIa:IXa) complex is formed on the activated platelet surface, it can activate platelet-bound X to Xa (this is a second mechanism for Xa activation in addition to its activation by TF:VIIa on the subendothelium). A Xa molecule can bind with a platelet-bound Va molecule to form a prothrombinase (Va:Xa) complex on the platelet surface. Prothrombinase can activate platelet-bound prothrombin to the enzyme thrombin.
- Thrombin released from the activated platelet's surface activates other platelets. It also activates cofactor molecules Va and VIIIa both in the plasma and on the surface of activated surfaces. It converts fibrinogen into fibrin monomers that then polymerize into a fibrin gel. (In this paper, we do not model the conversion of fibrinogen to fibrin monomer or fibrin polymerization.)
- Upon a platelet's activation, specific binding sites become expressed on its surface for each of the zymogen/enzyme pairs IX/IXa, X/Xa and prothrombin/thrombinand for each of the inactive/active cofactor pairs V/Va and VIII/VIIIa. The quantity of these binding sites that are available controls the formation and/or activity of the platelet-bound enzyme complexes.
- Platelets can be activated by contact with the subendothelium (not shown) or by exposure to thrombin or ADP. A finite quantity of ADP is released by a platelet during a time interval following the platelet's activation.
- Several chemical inhibitors (ATIII, TFPI and APC) act on various species in the reaction network. A platelet adhering to the subendothelium inhibits the activity of the molecules on the portion of subendothelium it covers (not shown).
- All fluid-phase chemical species and unactivated platelets move with the fluid and diffuse relative to it (not shown).

- Activated platelets can bind to other activated platelets. A cluster of bound platelets generates resistance to the local fluid motion (not shown).

Numerous models of 'portions' of the above system have been presented (e.g. Anand *et al.*, 2003; Beltrami & Jesty, 2001; Bodnar & Sequeira, 2008; Ermakova *et al.*, 2005; Xu *et al.*, 2008, 2009; Lobanov & Starozhilova, 2005; Lobanova *et al.*, 2004; Zarnitsina *et al.*, 2001; Jones & Mann, 1994; Hockin *et al.*, 2002; Fogelson & Guy, 2004, 2008), but, to our knowledge, the only one that couples a comprehensive model of coagulation biochemistry to models of platelet deposition and flow is that introduced by Kuharsky & Fogelson (2001). The 'Kuharsky and Fogelson (KF) model' considers the physical and chemical platelet and coagulation events that occur in a thin layer, called the reaction zone, just above a small vascular injury. The KF model takes into account plasma-phase, subendothelial-bound and platelet-bound enzymes and zymogens as well as activated and unactivated platelets. All species in the reaction zone are assumed to be well mixed; each species is characterized by its concentration that is tracked in time using an ordinary differential equation. Advective and diffusive transport of fluid-phase species (chemicals and platelets) into or out of the reaction zone is modelled by a mass-transfer term in which the mass-transfer coefficient depends on flow and diffusion parameters.

Studies of the KF model revealed a sharp threshold in thrombin production in response to different densities of TF exposure and showed that the threshold level of TF and the concentration of thrombin produced were modified only moderately by large changes in the flow shear rate. The model studies provided kinetic explanations of the reduced thrombin production with hemophilia and thrombocytopenia. This work also led to the hypothesis that as platelets adhere to the subendothelium, they cover and so physically inhibit subendothelial-bound enzymes. This hypothesis was later given experimental support by studies conducted at the Nemerson lab (Hathcock & Nemerson, 2004), and the predicted threshold and its dependence on shear rate were seen experimentally in the Diamond lab (Okorie *et al.*, 2008). Studies of an extended version of the model (Fogelson & Tania, 2005) highlighted the role of physical factors (fluid flow and platelet deposition) in establishing the TF threshold and indicated that for small injuries (≈ 10 μm in length), flow-mediated dilution is a much more potent inhibitor than the well-studied chemical inhibitors TFPI and APC.

Because it describes a well-mixed system, the KF model is limited to describing events near small injuries. Furthermore, because of its simple treatment of flow, it cannot account for significant growth of a thrombus and the effect of this on local flow and transport.

2. Model

We present a model that overcomes the significant limitations of the KF model just described. While it is built largely on the same assumptions about the chemical and physical interactions as the KF model, the new model incorporates spatial variations (both along the vessel wall and perpendicular to it into the lumen) and explicitly models the growth of a thrombus and how this is coupled with the local fluid dynamics. It also explicitly treats the platelet activating agonist ADP. The model we present below is fully extendable to 3D domains, but, so far, our studies of the model have been conducted in two-dimensions, so here, we describe the model in the setting of a 2D longitudinal slice of a segment of a vessel or a similar slice of a parallel plate flow chamber.

We consider a rectangular domain $[0, x_{\max}] \times [0, y_{\max}]$ in which the top and bottom vessel walls are represented by $y = 0$ and $y = y_{\max}$, respectively, and we assume that blood enters at $x = 0$ with a specified velocity profile and leaves at $x = x_{\max}$. A section of the bottom wall $x_1 < x < x_2$ is taken to represent subendothelial material exposed by vessel injury. Fluid and blood-borne species (chemicals and cells) may be present anywhere in the domain. Their concentrations at the upstream boundary $x = 0$

are set to their normal blood concentrations. We track four groups of platelets: mobile and unactivated, mobile and activated, bound and activated, and subendothelial bound and activated. Mobile platelets are advected by the fluid and diffuse through it. They may bind to the subendothelium or, if activated, to already bound and activated platelets of either type. We distinguish between three types of chemical species: fluid-phase chemicals, which advect with the fluid and diffuse through it; chemicals bound to the subendothelium, which are immobile as long as they remain bound and chemicals bound to bound platelets, which also are immobile while they remain bound to the platelets.

Although platelets are described in the model in terms of number densities (number/volume), the size of a platelet enters into the model in several ways. One is in terms of a maximum number density for platelets, $P_{\max}$, which we set to 6.67×10^7 platelets per mm^3 based on the assumption that 20 platelets fit tightly into 300 μm^3. The total platelet fraction $\phi^{\mathrm{T}}(\mathbf{x}, t)$ is the ratio of the sum of the four platelet number densities at $\mathbf{x}$ to this maximum density. The bound platelet fraction $\phi^{\mathrm{B}}(\mathbf{x}, t)$ is similarly the ratio of the sum of bound activated and subendothelium-bound activated platelet number densities to the maximum density. The bound platelet fraction ϕ^{B} determines the resistance to flow in the corresponding portion of a thrombus. The total platelet fraction ϕ^{T} in a piece of the thrombus determines how easily, if at all, platelets may move into that piece of thrombus. Platelets may be excluded from regions into which the fluid can move if ϕ^{T} is sufficiently high. Platelet size also enters through a variable η, which determines a region around the thrombus in which mobile activated platelets are deemed sufficiently close to bound platelets to bind. Finally, through the parameter $k_{\mathrm{adh}}(\mathbf{x})$, the size of a platelet determines the region in which a platelet is sufficiently close to the subendothelium to adhere to it. These manifestations of platelet size are discussed further below.

2.1 *Fluid*

We assume that the fluid motion is described by a modified version of the Navier–Stokes equations for incompressible viscous flow:

$$\rho\,(\,\mathbf{u}_t + \mathbf{u}\cdot\nabla\mathbf{u}\,) = -\nabla p + \mu\,\Delta\mathbf{u} \;-\; \mu\,\alpha(\phi^{\mathrm{B}})\,\mathbf{u}, \tag{2.1}$$

$$\nabla\cdot\mathbf{u} = 0. \tag{2.2}$$

Here, $\mathbf{u}(\mathbf{x}, t)$ and $p(\mathbf{x}, t)$ are the fluid velocity and pressure, respectively, at location $\mathbf{x}$ at time t; ρ is the fluid mass density and μ the dynamic viscosity. The term $-\mu\,\alpha(\phi^{\mathrm{B}})$, called the Brinkman term, is the modification we make to the standard Navier–Stokes equations. It represents frictional resistance to the fluid motion past point $\mathbf{x}$ due to bound platelets there and relates to the inverse permeability of the growing platelet mass. In this term, $\phi^{\mathrm{B}}(\mathbf{x}, t)$ is the bound platelet fraction defined earlier, and the frictional resistance is assumed to increase with $\phi^{\mathrm{B}}(\mathbf{x}, t)$ according to the function $\alpha(\phi^{\mathrm{B}}) = \alpha_{\max}\,(\phi^{\mathrm{B}})^2/((\phi_0^{\mathrm{B}})^2 + (\phi^{\mathrm{B}})^2)$. We set $\phi_0^{\mathrm{B}} = 0.5$ to be the bound platelet fraction at which the frictional resistance reaches half of its maximum value. We set $\alpha_{\max}$ sufficiently large that there is little flow through a thrombus with $\phi^{\mathrm{B}} \approx 1$.

To supplement these equations, there are no-slip boundary conditions on the top and bottom (vessel walls), a prescribed Poiseuille inflow at the left boundary and homogeneous Neumann outflow at the right boundary.

2.2 *Platelets*

We denote by $P^{\mathrm{m,u}}$, $P^{\mathrm{m,a}}$, $P^{b,a}$ and $P^{se,a}$ the number densities of four classes of platelets we track mobile unactivated, mobile activated, platelet-bound activated and subendothelium-bound activated,

respectively. Each of the these is a function of $\mathbf{x}$ and t, and their evolution equations are as follows:

$$\frac{\partial P^{\mathrm{m,u}}}{\partial t} = \underbrace{-\nabla \cdot \{\, W(\phi^{\mathrm{T}})\, (\mathbf{u}\, P^{\mathrm{m,u}} - D\, \nabla P^{\mathrm{m,u}})\, \}}_{\text{Transport by advection and 'diffusion'}} \tag{2.3}$$

$$\underbrace{-k_{\mathrm{adh}}(\mathbf{x})\, \{P_{\max} - P^{\mathrm{se,a}}\}\, P^{\mathrm{m,u}}}_{\text{Adhesion to subendothelium}} \underbrace{- \{A_1(e_2) + A_2([\mathrm{ADP}])\} P^{\mathrm{m,u}}}_{\text{Activation by thrombin or ADP}},$$

$$\frac{\partial P^{\mathrm{m,a}}}{\partial t} = -\nabla \cdot \{\, W(\phi^{\mathrm{T}})(\mathbf{u}\, P^{\mathrm{m,a}} - D\, \nabla P^{\mathrm{m,a}})\, \} - k_{\mathrm{adh}}(\mathbf{x}) \{P_{\max} - P^{\mathrm{se,a}}\} P^{\mathrm{m,a}} \tag{2.4}$$

$$+ \{A_1(e_2) + A_2([\mathrm{ADP}])\} P^{\mathrm{m,u}} \; - \; \underbrace{k_{\mathrm{coh}}\, g(\eta)\, P_{\max}\, P^{\mathrm{m,a}}}_{\text{Cohesion to bound platelets}},$$

$$\frac{\partial P^{\mathrm{b,a}}}{\partial t} = -k_{\mathrm{adh}}(\mathbf{x})\, (P_{\max} - P^{\mathrm{se,a}})\, P^{\mathrm{b,a}} \;\; + k_{\mathrm{coh}}\, g(\eta)\, P_{\max}\, P^{\mathrm{m,a}}, \tag{2.5}$$

$$\frac{\partial P^{\mathrm{se,a}}}{\partial t} = \;\; k_{\mathrm{adh}}(\mathbf{x})\, (P_{\max} - P^{\mathrm{se,a}})\, (P^{\mathrm{m,a}} + P^{\mathrm{m,u}} + P^{\mathrm{b,a}}). \tag{2.6}$$

For the mobile unactivated platelets, the term $\mathbf{J}^{\mathrm{m,u}} = \mathbf{u}P^{\mathrm{m,u}} - D\nabla P^{\mathrm{m,u}}$ is the flux of these platelets due to advection with the fluid and diffusion. Real platelets have size and may not move as readily as fluid through a region already occupied in part by thrombus-bound platelets. To account for this in our model, which tracks only the number density of platelets, not individual platelets of finite size, we multiply the flux vector $\mathbf{J}^{\mathrm{m,u}}$ by a function $W(\phi^{\mathrm{T}})$, which is a monotonically decreasing function of the total platelet fraction with $W(0) = 1$ and $W(1) = 0$. We used the specific function $W(\phi^{\mathrm{T}}) = \tanh(\pi(1 - \phi^{\mathrm{T}}))$, which is depicted in Fig. 2. In using this shape of function, we have assumed that the ability of mobile platelets to move into a region is only gradually impaired until ϕ^{T} reaches approximately 0.5 and then drops quickly. This limitation on advective and diffusive motion is imposed on both populations of mobile platelets.

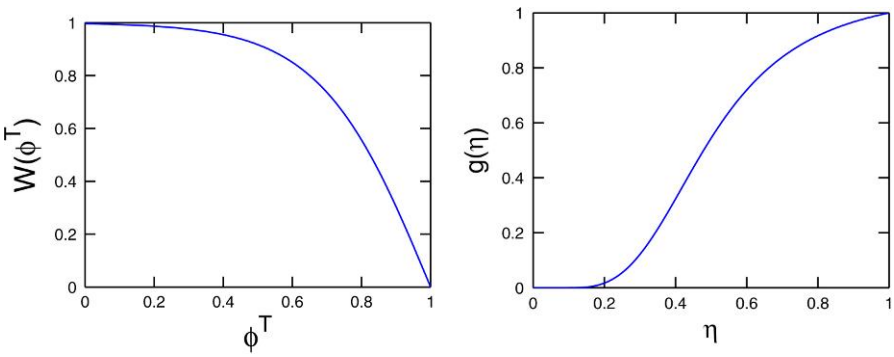

FIG. 2. Left: Platelet density-dependent mobility limitation function. Right: Binding affinity function $g(\eta)$.

The second term in each of equations (2.3) and (2.4) describes platelet adhesion to the exposed subendothelial material. The parameter $k_{\text{adh}}(\mathbf{x})$ is assumed to be a positive constant for points $\mathbf{x}$ within one platelet diameter's distance of the subendothelium and zero elsewhere. Since $P_{\max}$ is the maximum number density of platelets, $P_{\max} - P^{\text{se,a}}$ indicates the portion of the space just over the injury available for platelets to bind to the subendothelium. The rate of binding is assumed to be proportional to this value and to the local density of platelets that are sufficiently close to the subendothelium to be able to bind to it.

The third group of terms on the right-hand side of (2.3) and (2.4) account for the activation of platelets by the chemical agonists thrombin and ADP. The activation rate functions $A_1(e_2)$ and $A_2([\text{ADP}])$ are each assumed to have the form $k_c^{\text{pla}} \frac{c}{c^*+c}$, where c is the agonist concentration and k_c^{pla} and c^* are positive constants.

Equation (2.4) has one additional term that models platelet–platelet cohesion. Mobile activated platelets are able to bind to bound activated platelets to which they are sufficiently close and should bind at a rate that depends on the number of nearby bound activated platelets. We use the function $\eta(\mathbf{x}, t)$ to indicate both proximity to bound platelets and the density of nearby bound platelets. The function η is required to satisfy the partial differential equation:

$$\frac{\partial \eta}{\partial t} = D_\eta \, \Delta \, \eta - \gamma \, \eta + \gamma \left(\frac{P^{\text{b,a}} + P^{\text{se,a}}}{P_{\max}} \right). \tag{2.7}$$

The virtual substance η is produced by bound platelets at rate γ, decays at the same rate and diffuses with diffusion coefficient D_η. The value of η drops substantially over a distance $(D_\eta/\gamma)^{1/2}$ from the thrombus-bound platelets. We choose D_η and γ so that this distance is comparable to a platelet diameter. By using the same rate constant γ in both the production and the decay terms in the equation for η, at steady state, the level of η should be approximately the concentration of bound platelets in locations where there are bound platelets. The function η is used in the model solely to indicate for any location $\mathbf{x}$ how many bound platelets are nearby. We assume that the rate at which activated platelets bind is proportional both to their own concentration and to the value of the 'binding affinity' function $g(\eta)$ shown in Fig. 2: $g(\eta) = g_0 \max(0, (\eta - \eta_t)^3/(\eta_*^3 + (\eta - \eta_t)^3))$, where η_t is a threshold level below which there is no binding, $\eta_* + \eta_t$ indicates the value of η for which $g(\eta)$ changes rapidly and g_0 is chosen so that $g(1) = 1$. The terms in the equations for $P^{\text{b,a}}$ and $P^{\text{se,a}}$ are similar to those already described.

The full set of chemical equations that comprise the model are given in the Appendix, as are values of the rate constants and the sources of these values. In the next few sections, we illustrate the types of chemical equations that appear in the full model. In this discussion, we use the following notation: for zymogen i and enzyme i, Z_i and E_i, Z_i^{se} and E_i^{se} and Z_i^{m} and E_i^{m} refer to these proteins in the fluid, bound to the subendothelium or bound to the membrane of activated platelets, respectively. For example, E_7^{se} refers to the TF:VIIa complex on the subendothelium and E_5^{m} refers to factor Va bound to the platelet surface. Concentrations are denoted in a similar way but with lowercase z and e. A complex of Z_i and E_j is denoted by $Z_i{:}E_j$ and its concentration by $[Z_i{:}E_j]$. Special symbols are used for the platelet-bound 'tenase' VIIIa:IXa and 'prothrombinase' Va:Xa complexes, TEN = VIIIa:IXa and PRO = Va:Xa and [TEN] and [PRO] denote their respective concentrations. The inhibitors are denoted as APC and TFPI and their concentrations are denoted as [APC] and [TFPI]. We denote the complex of TFPI and Xa by TFPIa, because this is the 'active' form of the inhibitor, and its concentration by [TFPIa].

2.3 *Platelet-bound chemical species*

We now illustrate the different types of terms that appear in the model's equations for chemical species bound to activated platelets. To do this, we consider the equation for the platelet-bound enzyme E_2^{m} (thrombin).

$$\begin{aligned}\frac{\partial e_2^m}{\partial t} = &\underbrace{k_{e_2}^{on}\, e_2\, \left(N_2^b\, P^{b,a} + N_2^{se}\, P^{se,a} - z_2^{mtot} - e_2^{mtot}\right) - k_{e_2}^{off}\, e_2^m}_{\text{Binding with receptors on platelet surface}} \\ &+ \underbrace{(k^-_{z_5^m:e_2^m} + k^{cat}_{z_5^m:e_2^m})\, [Z_5^m{:}E_2^m] - k^+_{z_5^m:e_2^m}\, z_5^m\, e_2^m}_{\text{Activation of Va by thrombin}} \\ &+ \underbrace{(k^-_{z_8^m:e_2^m} + k^{cat}_{z_8^m:e_2^m})\, [Z_8^m{:}E_2^m] - k^+_{z_8^m:e_2^m}\, z_8^m\, e_2^m}_{\text{Activation of VIIIa by thrombin}} \\ &+ \underbrace{k^{cat}_{z_2^m:PRO}\, [Z_2^m{:}\mathrm{PRO}]}_{\text{Activation by prothrombinase}}\end{aligned} \tag{2.8}$$

The term $k_{e_2}^{\mathrm{on}}\, e_2\, (N_2^{\mathrm{b}} P^{\mathrm{b,a}} + N_2^{\mathrm{se}} P^{\mathrm{se,a}} - z_2^{\mathrm{mtot}} - e_2^{\mathrm{mtot}})$ gives the rate at which the fluid-phase enzyme thrombin binds to the specific binding sites for prothrombin and thrombin on the surfaces of activated platelets, while $k_{e_2}^{\mathrm{off}}\, e_2^{\mathrm{m}}$ is the rate at which thrombin dissociates from the binding sites. The quantities N_2^{b} and N_2^{se} denote the total number of binding sites per platelet specific for thrombin and prothrombin for each type of bound platelet, so that $N_2^{\mathrm{b}}\, P^{\mathrm{b,a}}$ and $N_2^{\mathrm{se}}\, P^{\mathrm{se,a}}$ are the volume concentrations of binding sites for those chemicals on the platelet-bound and subendothelium-bound platelets, respectively. The concentration of occupied binding sites $z_2^{\mathrm{mtot}} + e_2^{\mathrm{mtot}}$ is subtracted from this quantity to give the concentration of available binding sites. The concentrations of occupied binding sites account for platelet-bound prothrombin and thrombin as well as with their platelet-bound complexes: $z_2^{\mathrm{mtot}} = z_2^{\mathrm{m}} + [Z_2^{\mathrm{m}}{:}\mathrm{PRO}]$ and $e_2^{\mathrm{mtot}} = e_2^{\mathrm{m}} + [Z_5^{\mathrm{m}}{:}E_2^{\mathrm{m}}] + [Z_8^{\mathrm{m}}{:}E_2^{\mathrm{m}}]$. The terms $\left(k^-_{z_5^m:e_2^m} + k^{cat}_{z_5^m:e_2^m}\right)[Z_5^{\mathrm{m}}{:}E_2^{\mathrm{m}}]$ and $k^+_{z_5^m:e_2^m}$ pertain to the association and dissociation of Z_5^{m} with E_2^{m} on the platelet surface and the enzymatic activation of Z_5^{m} to E_5^{m}. The terms $\left(k^-_{z_8^m:e_2^m} + k^{cat}_{z_8^m:e_2^m}\right)[Z_8^{\mathrm{m}}{:}E_2^{\mathrm{m}}] - k^+_{z_8^m:e_2^m}\, z_8^{\mathrm{m}}\, e_2^{\mathrm{m}}$ play a similar role, but for Z_8^{m}. Platelet-bound chemicals are considered only in locations where $P^{\mathrm{b,a}}$ or $P^{\mathrm{se,a}}$ is nonzero.

2.4 *Subendothelium-bound chemical species*

We use the equation for the concentration, e_7^{se}, of the enzyme complex TF:VIIa to illustrate the terms that appear in equations for chemical species bound to the subendothelium:

$$\begin{aligned}\frac{\partial e_7^{se}}{\partial t} = &\underbrace{k_{e_7}^{on}\, e_7\, (TF - e_7^{se,tot} - z_7^{se,tot}) - k_{e_7}^{off}\, e_7^{se}}_{\text{Binding with TF}} \\ &+ \underbrace{k^{cat}_{z_7^{se}:e_{10}}\, [Z_7^{se} : E_{10}] + k^{cat}_{z_7^{se}:e_2}\, [Z_7^{se} : E_2]}_{\text{Activation by Xa or thrombin}}\end{aligned} \tag{2.9}$$

$$+\underbrace{(k^{-}_{z_{10}:e^{se}_7}+k^{cat}_{z_{10}:e^{se}_7})\,[Z_{10}:E^{se}_7]-k^{+}_{z_{10}:e^{se}_7}\,z_{10}\,e^{se}_7}_{\text{Activation of X to Xa}}$$

$$+\underbrace{(k^{-}_{z_9:e^{se}_7}+k^{cat}_{z_9:e^{se}_7})\,[Z_9:E^{se}_7]-k^{+}_{z_9:e^{se}_7}\,z_9\,e^{se}_7}_{\text{Activation of IX to IXa}}$$

$$+\underbrace{k^{-}_{tfpia:e^{se}_7}\,[\text{TFPIa}:E^{se}_7]-k^{+}_{tfpia:e^{se}_7}\,[\text{TFPIa}]\,e^{se}_7}_{\text{Binding with TFPI:Xa}}$$

$$-\underbrace{k_{adh}(\mathbf{x})\,(P^{se,a}+P^{se,u}+P^{b,a})\,e^{se}_7}_{\text{Coverage by Platelet Deposition}}$$

As indicated by the labels under the terms, the first five groups of terms describe the binding of fluid-phase factor VIIa molecules to available TF molecules or the unbinding of VIIa from TF; the activation of TF:VII to TF:VIIa by factor Xa or thrombin; the binding of factor X to TF:VIIa and its unbinding from or activation by this complex; the binding of factor IX to TF:VIIa an its unbinding from or activation by the complex; and the interaction of the inhibitor complex TFPIa (i.e. TFPI:Xa) with TF:VIIa. The only new type of term is the last one that describes the decrease of accessible TF:VIIa molecules at a rate proportional to the rate at which platelets become subendothelium-bound and thus cover a portion of the subendothelium. A similar platelet deposition term appears in each of the subendothelium-bound chemical equations

2.5 *Fluid-phase chemical species*

Each of the fluid-phase chemicals advects with the fluid and diffuses through it. Some fluid-phase chemicals bind to bound platelets and some bind to the subendothelium. We use fluid-phase factor Xa to illustrate the types of terms that appear in the differential equations and boundary conditions for fluid-phase chemicals:

$$\frac{\partial e_{10}}{\partial t}=\underbrace{-\mathbf{u}\cdot\nabla e_{10}+\nabla\cdot(D\nabla e_{10})}_{\text{Transport by advection and diffusion}} \tag{2.10}$$

$$+\underbrace{(k^{-}_{z_7:e_{10}}+k^{cat}_{z_7:e_{10}})[Z_7:E_{10}]\;-\;k^{+}_{z_7:e_{10}}\,z_7\,e_{10}}_{\text{Activation of VII}}$$

$$\underbrace{-\,k^{in}_{e_{10}}\,e_{10}\;+\;k^{-}_{tfpi:e_{10}}\,[\text{TFPIa}]\;-\;k^{+}_{tfpi:e_{10}}\,[\text{TFPI}]\,e_{10}}_{\text{Inhibition by ATIII or by binding to TFPI}}$$

$$\underbrace{-\,k^{on}_{e_{10}}\,e_{10}\,\left(N^{b}_{10}P^{b,a}+N^{se}_{10}P^{se,a}-z^{ptot}_{10}-e^{ptot}_{10}\right)+k^{off}_{e_{10}}\,e^{m}_{10}}_{\text{Binding to platelet receptor for X and Xa}}$$

The first group of terms on the right-hand side of this equation represent advection and diffusion. The next group of terms concerns activation of fluid-phase factor VII by fluid-phase factor Xa. The third group has a term $-\,k^{in}_{e_{10}}\,e_{10}$ representing inhibition of factor Xa by the fluid-phase inhibitor ATIII, and a set of terms describing the interaction of factor Xa with the fluid-phase inhibitor TFPI. The

last group of terms represents binding and unbinding of Xa with the platelet surface receptors shared by factors X and Xa. Similarly to the discussion of platelet-bound thrombin above, $N_{10}^{\mathrm{b}} P^{\mathrm{b,a}} + N_{10}^{\mathrm{se}} P^{\mathrm{se,a}} - z_{10}^{\mathrm{ptot}} - e_{10}^{\mathrm{ptot}}) + k_{e_{10}}^{\mathrm{off}}\, e_{10}^{\mathrm{m}}$ is the total concentration of platelet binding sites for X/Xa, $N_{10}^{\mathrm{b}} P^{\mathrm{b,a}} + N_{10}^{\mathrm{se}} P^{\mathrm{se,a}}$, less the concentration of those already occupied by either X or Xa, $z_{10}^{\mathrm{ptot}} + e_{10}^{\mathrm{ptot}}$.

For a fluid-phase chemical that can be produced on the subendothelium and that can bind to molecules on the subendothelium, these interactions are incorporated in the boundary condition for that chemical's concentration. For e_{10}, the boundary condition at each point of the injured portion of the vessel wall is

$$-D\frac{\partial e_{10}}{\partial y} = \underbrace{k^{cat}_{z_{10}:e_7^{se}}\,[Z_{10}{:}E_7^{se}]}_{\text{Activation by TF:VIIa}} + \underbrace{\left(k^{-}_{z_7^{se}:e_{10}} + k^{cat}_{z_7^{se}:e_{10}}\right)[Z_7^{se}{:}E_{10}] - k^{+}_{z_7^{se}:e_{10}}\, z_7^{se}\, e_{10}}_{\text{Binding to and activation of TF:VII}} \tag{2.11}$$

while on the remaining portions of the vessel walls, the boundary condition is

$$-D\frac{\partial e_{10}}{\partial y} = 0. \tag{2.12}$$

As indicated earlier, the concentration of a fluid-phase chemical such as factor Xa is set to its normal plasma concentration at the upstream end of the domain and is assumed to satisfy the condition $\partial e_{10}/\partial x = 0$ at the downstream boundary.

2.5.1 *ADP.* An unactivated platelet contains quantities of the activating chemical ADP stored within its dense granules. Upon activation, the dense granules fuse with the platelet's membrane and release their contents into the surrounding fluid. To represent this, we assume that ADP is released over a period of 1–5 s after platelet activation. Once released, ADP molecules move through the fluid and can activate nearby platelets. Embodying these assumptions, the ADP concentration, [ADP], satisfies the equation

$$\frac{\partial[\mathrm{ADP}]}{\partial t} = -\mathbf{u}\cdot\nabla[\mathrm{ADP}] + \nabla\cdot(D\nabla[\mathrm{ADP}]) + \sigma_{\mathrm{release}}, \tag{2.13}$$

which says that ADP moves by advection and diffusion. The source term $\sigma_{\mathrm{release}}$ describes the release of ADP from bound activated platelets.

We define the source term from ADP release as

$$\sigma_{\mathrm{release}}(\mathbf{x}, t) = \int_0^\infty \hat{A}R(\tau)\frac{\partial}{\partial t}(P^{\mathrm{b,a}} + P^{\mathrm{se,a}})(\mathbf{x}, t-\tau)\mathrm{d}\tau, \tag{2.14}$$

where $\hat{A}$ is the total quantity of ADP released by an activated platelet and $R(\tau)$ is the rate of release at an 'elapsed time' τ since the platelet was activated, normalized so that $\int_0^\infty R(\tau)\mathrm{d}\tau = 1$. To understand (2.14), note that $\frac{\partial}{\partial t}(P^{\mathrm{b,a}} + P^{\mathrm{se,a}})(\mathbf{x}, t-\tau)\mathrm{d}\tau$ is the number of platelets newly activated and bound at location $\mathbf{x}$ in the time interval $[t-\tau, t-\tau+\mathrm{d}\tau]$ and that $\hat{A}R(\tau)$ is the rate of release of ADP by these platelets τ time units later, i.e. at time t. We choose $R(\tau)$ to have value 0 up to 1 s after activation, to be a positive bell-shaped function for times $1 < \tau < 5$ s and to have a peak at 3 s, consistent with observations reported in the literature (Reed *et al.*, 2000). Since $R(\tau)$ is nonzero only in the interval $0 < \tau < 5$ s, formula (2.14) actually involves an integral over that finite time interval.

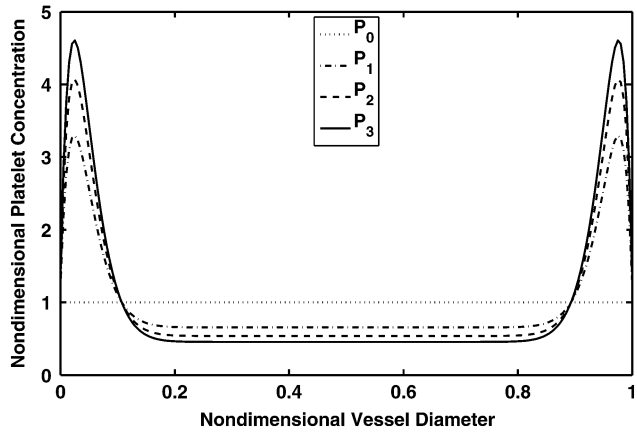

FIG. 3. Platelet inlet concentration profiles. Peak-to-centre ratios are set to approximately 1, 5, 7.5 and 10 for platelet profiles P_0, P_1, P_2 and P_3, respectively.

2.6 *Near-wall excess of platelets*

Observations *in vivo* (Tangelder *et al.*, 1985) found that the near-wall platelet concentration in arterioles can be two to three times higher than that in the centre of the vessel and *in vitro* experiments demonstrated with platelet-sized beads that the near-wall concentration can be three to eight times that in the central region, depending on wall shear rate and hematocrit (Eckstein *et al.*, 1988). Based on his observations, Eckstein (Eckstein & Belgacem, 1991) presented a concentration profile function that is the basis for the inlet profile we prescribe for mobile unactivated platelets. Figure 3 shows the four inlet platelet concentration profiles that result from our synthesis of data in Eckstein *et al.* (1988), Tilles & Eckstein (1987) and Yeh *et al.* (1994) and that we used in our simulations.

2.7 *Numerical methods*

We solve the model equations in a rectangular spatial region $R = [0, x_{\max}] \times [0, y_{\max}]$. For all the variables, including the fluid, we use a uniform mesh placed over R with equal mesh spacing in both the x and y directions. For each differential equation, we use a finite-difference approximation defined at points on this mesh. During each time step of the computation, we perform the following series of updates for the unknowns:

1. The discretized Navier–Stokes equations with Brinkman term are solved using a second-order projection method, details of which can be found in Leiderman *et al.* (2008), to give new fluid velocities u, v and pressure p.
2. Platelets activated within the previous time step are counted and the ADP release function, σ_{release}, is updated.
3. Mobile platelets and fluid-phase chemicals are updated to account for advection using LeVeque's high-resolution advection algorithm (LeVeque, 1996).
4. Mobile platelets, fluid-phase chemicals and η are updated to account for diffusion using a Crank–Nicolson time discretization and the usual spatial-difference approximation to the Laplacian.
5. All species are updated to account for reactions using a second-order Runge–Kutta solver.

6. The platelet fractions of bound platelets, ϕ^{B} and ϕ^{T}, are calculated and $\alpha(\phi^{\mathrm{B}})$ and $W(\phi^{\mathrm{T}})$ are updated.
7. Repeated until desired time.

The simulations described below were carried out on a 32×128 grid and with a variable time step set to three-fourths of the Courant number. For simulations carried out on a 64×256 grid, the bound platelet and thrombin concentrations after 600 s were very similar to those shown.

3. Results

Figure 4 shows 12 snapshots from a simulation of 10 min of clotting activity. Blood flows from left to right with a prescribed parabolic inflow velocity profile. Platelets and fluid-phase clotting chemicals have prescribed concentrations at the inlet and move downstream with the flow. The channel has height 60 μm, length 240 μm and there is an injury of length 90 μm centred at the midpoint of the bottom wall. (This is the setup for all the simulations reported in this paper.) The initial TF density in the injury is set to 15 fmol cm^{-2}. After 50 s, platelets partially cover the injury site, but there is little effect as yet on the overall flow. As the thrombus grows beyond the initial subendothelial-bound platelets, it begins to noticeably perturb the flow. By 600 s, the thrombus has grown substantially and, as indicated by the uneven distribution of dark red patches, the platelet distribution in the thrombus has significant spatial heterogeneity. The flow has been largely diverted around the thrombus accelerating as it passes over the thrombus and then slowing when the vessel lumen widens downstream of the thrombus. The velocity within the thrombus is much less than that in the bulk flow but has a significant impact on thrombus growth as discussed below.

3.1 *Thrombin production dependence on TF density*

Figure 5 shows that the concentration of thrombin that is obtained after 10 min of clotting activity has a sharp threshold dependence on the density of TF initially exposed to the blood. This prediction is in agreement with results from the well-mixed KF model (Kuharsky & Fogelson, 2001; Fogelson & Tania, 2005). The threshold behaviour can also be seen in the thrombin concentration distribution and in the accumulation of bound platelets for different initial TF exposures as also shown in Fig. 5. For a TF density of 1 fmol cm^{-2}, thrombin production is insignificant, while for a slightly larger TF density

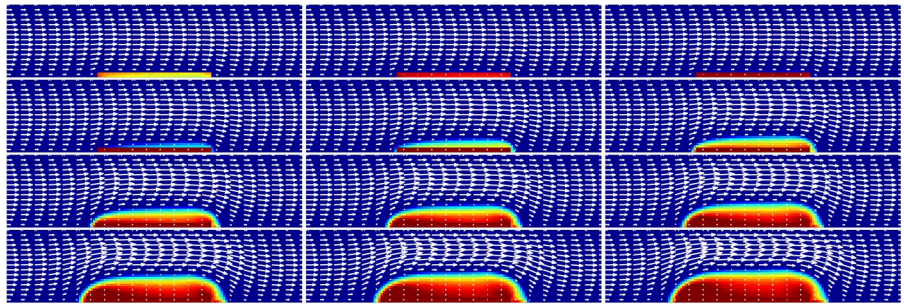

FIG. 4. Time sequence of growing thrombus at times 50, 100, 150, ..., 600 s (from left to right, top to bottom) for initial TF density of 15 fmol cm^{-2}, shear rate of 1500 s^{-1} and platelet profile of P_3. The arrows show the fluid velocity and have a uniform scaling throughout the sequence. Bound platelet concentrations vary from 0 (dark blue) to $P_{\max}$ (dark red).

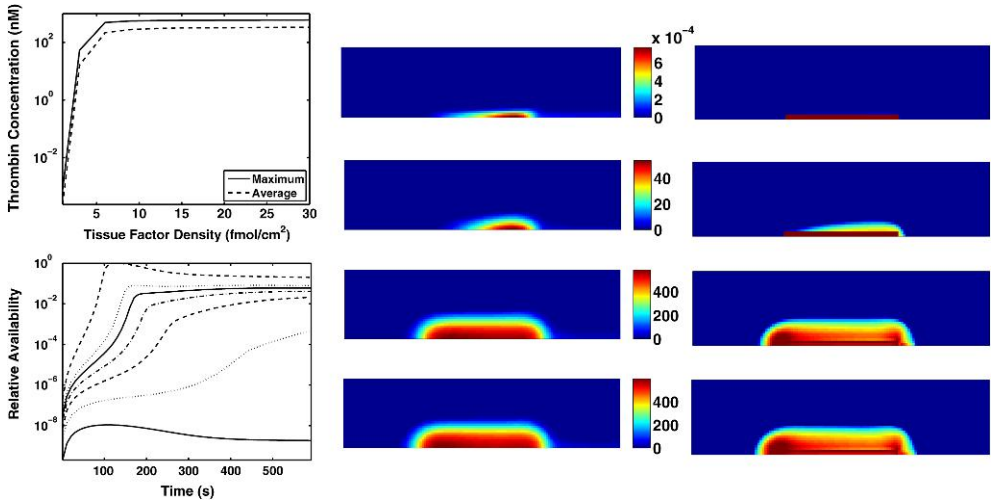

FIG. 5. The top-left plot shows the spatial maximum and mean thrombin concentrations within the thrombus 10 min after TF exposure as a function of the density of exposed TF. The bottom-left plot shows the relative simultaneous availability of e_9 and e_8^{m} as a function of time for TF densities (bottom to top) 1, 3, 6, 9, 12, 15 and 30 fmol cm^{-2}. The plots in columns 2 and 3 are the spatial concentrations of fluid-phase thrombin (e_2) in nanomolar and bound platelets ($P^{\mathrm{b,a}} + P^{\mathrm{se,a}}$) that vary from 0 (dark blue) to $P_{\max}$ (dark red). From top to bottom, the density of TF exposed is 1, 3, 15 and 30 fmol cm^{-2}. For all cases, the wall shear rate is 500 s^{-1} and the platelet profile is P_1.

of 3 fmol cm^{-2}, the thrombin concentration reaches levels of 10–50 nM. Once the TF exposure is sufficiently high, there is little change in the amount of thrombin produced or in the size of the thrombus that develops. This can be seen in the results for TF densities of 15 and 30 fmol cm^{-2} shown in the bottom two panels in the centre and right of Fig. 5.

Using an extension of the KF model, Fogelson & Tania (2005) showed that an insignificant amount of thrombin was produced if there was only a short 'overlap time' during which substantial amounts of fluid-phase IXa and platelet-bound VIIIa both existed. Both these concentrations depend on the level of TF exposure, factor IXa because it is produced by the TF:VIIa complex and platelet-bound VIIIa because the dominant activator of this cofactor during the first 60 s of clotting activity is factor Xa also produced by the TF:VIIa complex. Since the current model gives spatial information, we quantified the overlap time by summing, over all spatial points, the product of the fluid-phase IXa and the platelet-bound VIIIa concentrations. (We normalized this quantity by its maximum over all times and TF densities considered.) The curves in the bottom-left panel of Fig. 5 show this measure of overlap as a function of time for different TF densities (increasing from bottom to top) and we see that for all above threshold cases (curves 3 and higher), there is a period in which the overlap measure increases sharply. This sharp increase is followed quickly by successive sharp increases in tenase, prothrombinase and thrombin (not shown).

As the TF density increases from 15 to 30 fmol cm^{-2}, there is little change ($\approx$2.5%) in the maximum concentration of thrombin achieved. Since this level is substantially below the plasma concentration (1.4 μM) of the thrombin precursor, prothrombin, substrate availability is not the limiting factor that prevents greater thrombin production. The left panel of Fig. 6 shows how the maximum tenase and prothrombinase concentrations change with TF density. We see that the tenase concentration continues to increase significantly even at high TF densities, but the prothrombinase concentration plateaus. The increase in tenase implies an increased 'potential' to generate platelet-bound factor Xa, the enzyme part

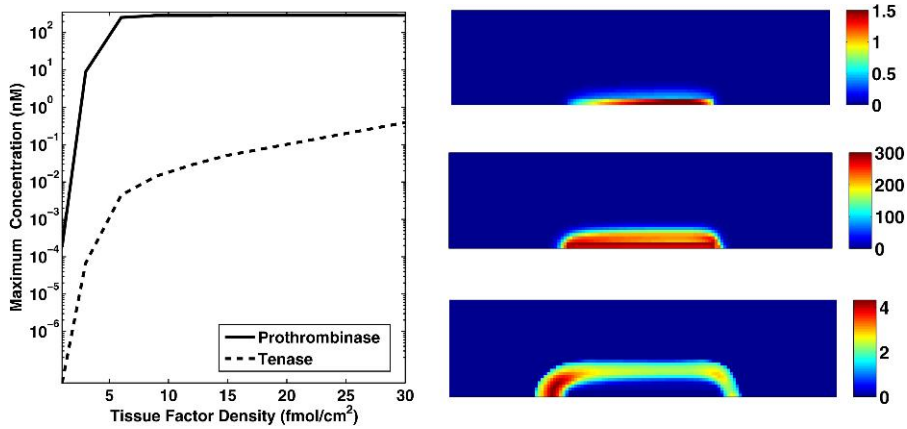

FIG. 6. Left: Maximum prothrombinase and tenase concentrations at any point within the entire domain 10 min after TF exposure to plasma as a function of the density of TF exposed. Wall shear rate of the flow was 500 s^{-1}. Right: Spatial concentration (nanomolar) of tenase, prothrombinase and available binding sites for factor X/Xa. The TF density is 15 fmol cm^{-2} and the wall shear rate is 500 s^{-1}.

of prothrombinase, and yet, there is little change in prothrombinase levels. The explanation for this is that tenase is unable to produce platelet-bound factor Xa at its potential. The right panels of Fig. 6 show, for a TF density of 15 fmol cm^{-2}, the spatial distribution (at 10 min) of the tenase and prothrombinase complexes and the unoccupied platelet binding sites for X and Xa. Where the tenase concentration is high, there are few unoccupied binding sites to which X can bind. Since tenase activates only platelet-bound X to Xa, tenase activity is therefore severely limited. The bulk of the occupied X/Xa binding sites are bound to Xa molecules that have been incorporated in prothrombinase complexes. Many X/Xa binding sites are available on newly activated platelets at the upstream end of the thrombus, but there is essentially no tenase in that region. The spatial distribution of tenase, empty X/Xa binding sites and prothrombinase for a TF density of 30 fmol cm^{-2} (not shown) are similar, but the tenase levels are about six-fold higher.

3.2 *Thrombus growth dependence on wall shear rate and near-wall excess of platelets*

Turitto *et al.* (1987) report an increase in thrombus growth with wall shear rate. They attributed this increase to an enhancement of the local arrival rate of platelets and hypothesized that a possible mechanism for such an enhancement would be a near-wall excess of platelets of the type illustrated in Fig. 3. Motivated by these experiments, we carried out simulations at three shear rates 500, 1000 and 1500 s^{-1} and with the four platelet concentration profiles P_0, P_1, P_2 and P_3 illustrated in Fig. 3. Results of these simulations are shown in Figs 7 and 8. One set of experiments, the 'uniform profile' set, looked at the effect of varying shear rate with the fixed and uniform inflow platelet concentration profile P_0. For the 'fixed nonuniform profile' set, the inflow platelet profile was kept fixed at the nonuniform profile P_1 with a peak-to-centre ratio of 5 as the shear rate was varied. In the 'varying nonuniform profile' experiments, the different spatially nonuniform inflow profiles P_1, P_2 and P_3, with peak-to-centre ratios of 5, 7.5 and 10, were used for shear rates 500, 1000 and 1500 s^{-1}, respectively.

From the spatial plots (at 600 s) in Fig. 7, we see (i) no apparent difference in the bound platelet concentration as shear rate is varied with the spatially uniform platelet profile, (ii) an increased extent of high-density regions (dark red) but no apparent difference in overall thrombus size as shear rate is

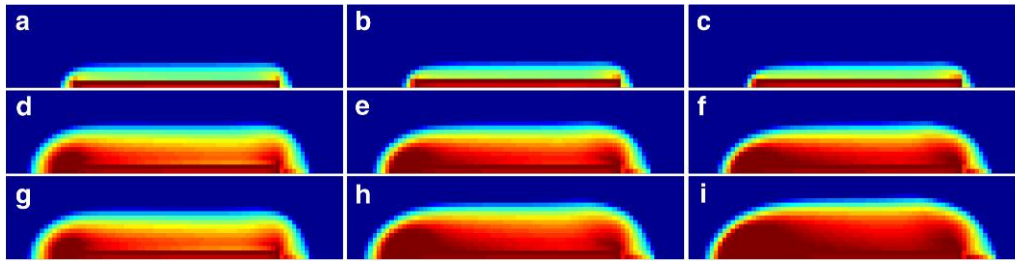

FIG. 7. Close-up of approximately 188 μm long by 38 μm high region around thrombus. Bound platelet concentrations after 10 min vary from 0 (dark blue) to $P_{\max}$ (dark red). Columns 1, 2 and 3 represent wall shear rates of 500, 1000 and 1500 s^{-1}, respectively. The experiments in rows 1 and 2 use platelet profiles P_0 and P_1, respectively. The experiments across the bottom row use the platelet profiles P_1, P_2 and P_3.

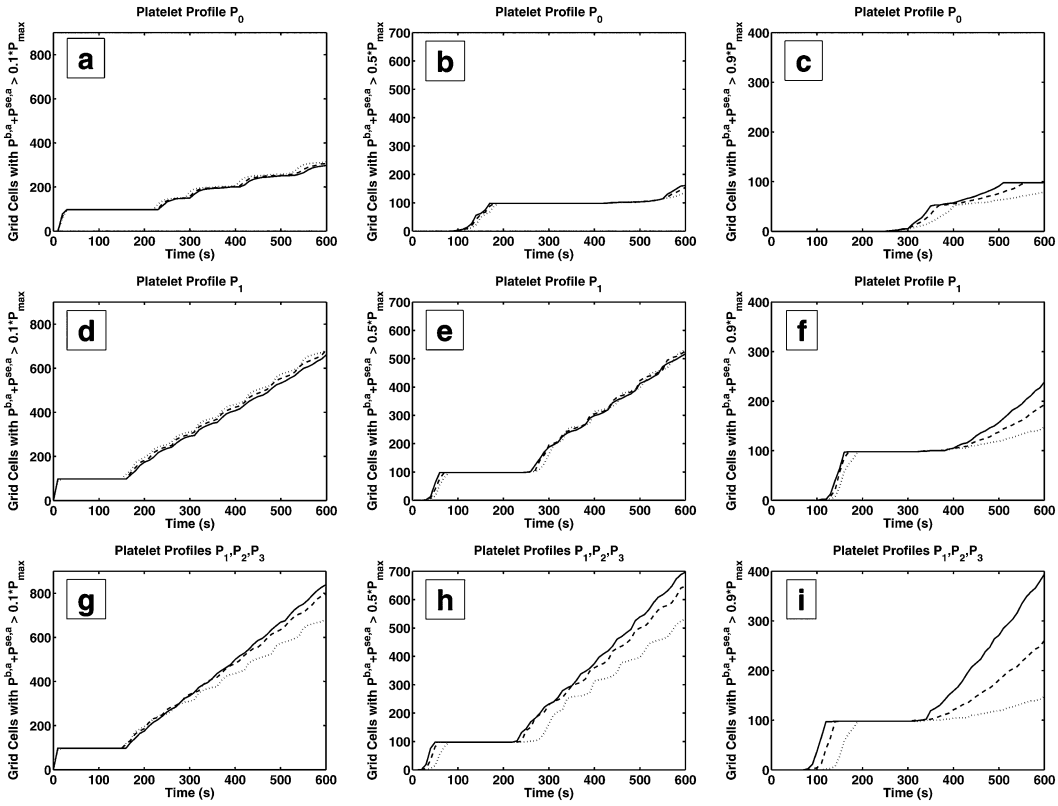

FIG. 8. Clot 'area' for each set of experiments: uniform platelet profiles (top row, a–c), fixed nonuniform platelet profiles (middle row, d–f) and varying nonuniform profiles (bottom row, g–i). In all cases, the dotted line, dash-dot line and solid line represent wall shear rates of 500, 1000 and 1500 s^{-1}, respectively.

increased in the fixed nonuniform simulations and (iii) an increase in both overall thrombus size and in high-density regions as shear rate increased in the varying nonuniform simulations. Comparing plots within each column, we see that for a fixed shear rate, thrombus size increased with increasing peak-to-centre ratios in platelet concentration.

To quantify these observations further, we computed for each clot, the 'area' in which the bound platelet concentration exceeded 10, 50 and 90% of $P_{\max}$, respectively. We regard the first as giving a measure of overall thrombus size, and the latter two as providing information about the bound platelet density distribution with the thrombus. (These areas were computed by counting the computational grid cells in which the various platelet density levels were exceeded.) The results are shown in Fig. 8.

A noteworthy feature of all the plots is the appearance of a temporary plateau at an area of 100 grid cells. This is the area of the region in which the adhesion rate function $k_{\text{adh}}(\mathbf{x})$ is nonzero. Recall that to adhere directly to the subendothelium does not require prior activation, so the time to reach this plateau is affected little by chemistry but can be affected by the rate of delivery of platelets to this region. This is clearly seen in Fig. 8(f and i), which shows how the time it takes for subendothelial platelets to reach 90% of their maximum concentration is affected by shear rate (Fig. 8f) or shear rate and platelet concentration profile together (Fig. 8i). The end of the plateaus in the left panels indicates the beginning of thrombus growth beyond direct subendothelial adhesion.

Each panel in the top two rows of Fig. 8 shows the effect of varying shear rate for a fixed inflow platelet concentration profile. The plots for 10 and 50% density show that the effect of shear rate alone on thrombus area is minimal. The 90% density plots demonstrate that shear rate affects thrombus density; platelet density in the thrombus increases with shear rate. Referring to Fig. 7, we see that the density increase occurs in a spatially heterogeneous manner. When the platelet peak-to-centre ratio and the shear rate are both increased (Fig. 8(g–i)), there is a moderate increase in thrombus area and a large increase in thrombus density compared both to the change in area in this set of experiments and to the density changes when shear rate only is varied (Fig. 8f). At the highest shear rate, large density regions developed in the upstream third and near the downstream end of the thrombus.

3.3 *Platelet activation by chemical agonists*

In the model, platelets can be activated by two fluid-phase chemical agonists, ADP and thrombin. To explore the importance of each activating mechanism at different times and locations, we tracked the following two quantities:

$$P_{\text{act}}^{e_2}(\mathbf{x}, t) = \int_{t-10}^{t} A_1(e_2(\mathbf{x}, t'))\, P^{\text{m,u}}(\mathbf{x}, t')\mathrm{d}t' \tag{3.1}$$

and

$$P_{\text{act}}^{\text{ADP}}(\mathbf{x}, t) = \int_{t-10}^{t} A_2([\text{ADP}](\mathbf{x}, t'))\, P^{\text{m,u}}(\mathbf{x}, t')\mathrm{d}t'. \tag{3.2}$$

Here, $P_{\text{act}}^{e_2}(\mathbf{x}, t)$ and $P_{\text{act}}^{\text{ADP}}(\mathbf{x}, t)$ (shown in Fig. 9 for t = 10, 120, 360, 480 and 600 s) are the number per unit volume of platelets activated at location $\mathbf{x}$ during the time interval $t - 10$ to t by thrombin and ADP, respectively. Activation by ADP dominates during early thrombus formation (up to about 150 s) before substantial thrombin is produced. Its effectiveness peaks during this period at about 20 s and then decreases. As the effect of ADP declines, that of thrombin grows because of increases in the thrombin concentration. Thrombin remains the dominant activator during the remainder of thrombus development, but the increased rate of platelet activation increases the rate of ADP release, which, in turn, causes a resurgence in ADP-induced activation, particularly at the upstream end of the thrombus.

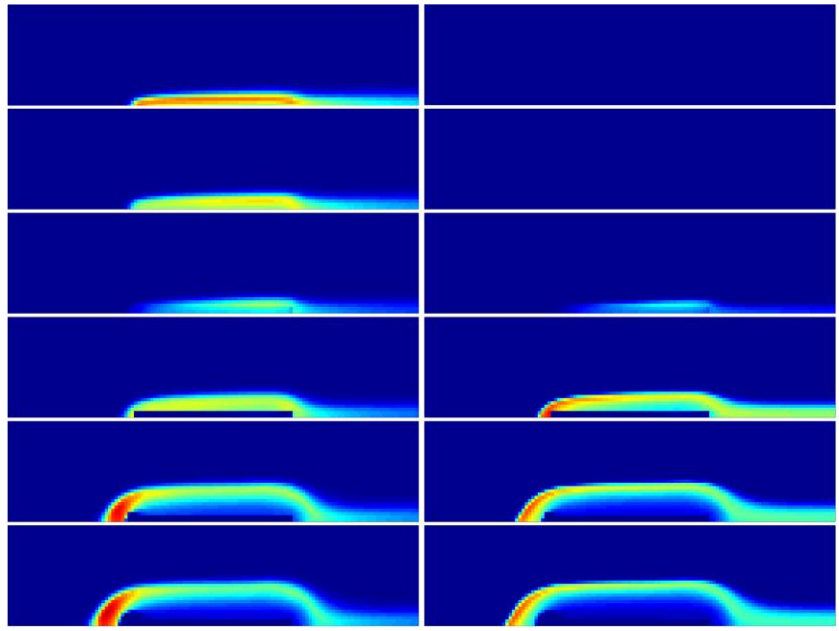

FIG. 9. Activation of platelets by ADP (left) and thrombin (right) in the previous 10-s interval. The rows from top to bottom are for times 10, 60, 150, 240, 480 and 600 s. The shear rateis 500 s^{-1}, the platelet profile is P_1 and the TF density is 15 fmol cm^{-2}. Platelet activation is shown in densities that range from 0 (dark blue) to 4 (dark red) times 10^4 platelets per mm^3 for ADP and 0 (dark blue) to 4 (dark red) times 10^5 platelets per mm^3 for thrombin.

3.4 *Transport in the thrombus*

As the thrombus grows, it offers more resistance to the flow and the bulk of the flow is diverted around the thrombus. But, because the thrombus is porous, fluid motion within the thrombus persists albeit at a velocity much less than that outside of the thrombus. As the first platelets adhere to the subendothelium, the velocity within the early thrombus becomes very small. As the thrombus grows and occludes more of the vessel, pressure builds up at the front edge of the thrombus and thus, the velocity of the fluid within the thrombus increases (see Fig. 10), reaching a magnitude on the order of 1–3 $\mu m\ s^{-1}$ (depending on shear rate). This is the velocity at which fluid-phase chemicals inside the thrombus advect. However, recalling the platelet-density-dependent limitation on platelet advection, platelets move at reduced velocities (see Fig. 11), in particular, where the density of bound platelets is high.

Although fluid velocities inside a partially developed thrombus are small relative to those in the bulk flow around the thrombus, they are large enough to potentially carry fluid-phase chemicals the entire length of the injury within 30–90 s (see Fig. 11). However, fluid-phase species may also be transported by diffusion. To explore the relative influence of advective and diffusive transport, we use the nondimensional Peclet number, $\mathrm{Pe} = uL/D$. We define a Peclet number at each point $\mathbf{x}$ in the thrombus using the magnitude of the velocity at that point, the species' diffusion coefficient D and the length $L = 90\ \mu m$ of the injury. The last column of Fig. 11 shows spatial plots of $1/\mathrm{Pe}(\mathbf{x}, t)$ and demonstrates that diffusion is more effective than flow at moving chemical species at certain times during the simulation. These plots do not give information about the 'direction' of movement, but, as we explain shortly, some of this

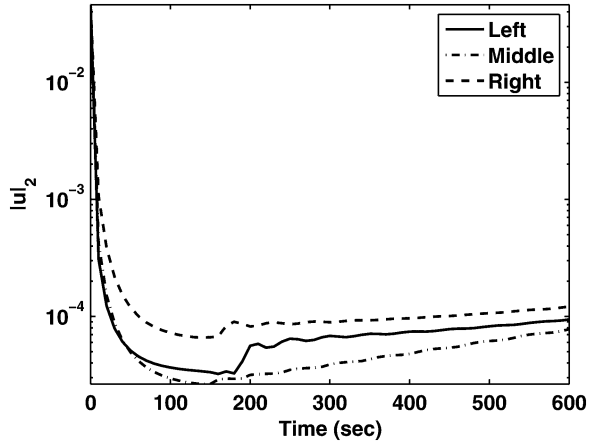

FIG. 10. Flow speed (cm s^{-1}) inside the thrombus approximately 1 μm from the vessel wall. The curves left, middle and right correspond to locations about 8 μm from the upstream end, at the middle and from the downstream end of the injury, respectively. The wall shear rate is 500 s^{-1}, the platelet profile is P_1 and the TF density is 15 fmol cm^{-2}.

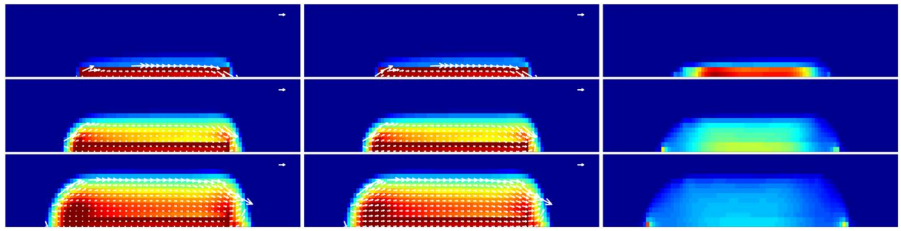

FIG. 11. Close-up of near thrombus region at times 200, 400 and 600 s (top to bottom). The left column shows platelet velocities and the middle column shows fluid velocities along with bound platelet concentrations. All velocity vectors are scaled relative to the 2 μm s^{-1} vector shown in the upper-right corner of the plots. The velocity vectors only appear in regions where the bound platelet concentration exceeds 1×10^7 platelets mm^{-3} and the nondimensional concentration of the virtual substance, η, exceeds 0.27. The right column shows the spatial distribution of $1/\mathrm{Pe}$. Bound platelet concentrations vary from 0 (dark blue) to $P_{\max}$ (dark red), and $1/\mathrm{Pe}$ varies from near 0 (dark blue) to 2 (dark red).

movement is indeed upstream against the direction of the flow. The velocities within the thrombus increase starting at about time 150 s (see Fig. 10), and the value of $1/\mathrm{Pe}$ and, with it, the relative influence of diffusion to advection decrease after that time.

The time at which $1/\mathrm{Pe}$ is highest (i.e. when the intrathrombus velocity is lowest) is crucial for the formation and spread upstream of the important platelet-bound enzyme complexes. Figure 12 shows spatial concentrations (nanomolar) of eight different platelet-bound chemical species that are vital to thrombin formation and, thus, thrombus growth. The columns in Fig. 12 are for times 140, 180 and 250 s, respectively. At 140 s, there are substantial amounts of the platelet-bound zymogens, Z_5^{m}, Z_8^{m} and Z_{10}^{m}, present everywhere within the thrombus. A small quantity of platelet-bound thrombin (E_2^{m}) can be seen in the downstream portion of the thrombus in the region where prothrombinase (PRO) is present. The enzyme E_9^{m}, which only appears when the activated fluid-phase enzyme E_9 (IXa) binds weakly to platelets, is also found in the downstream region. The small amount of thrombin is apparently

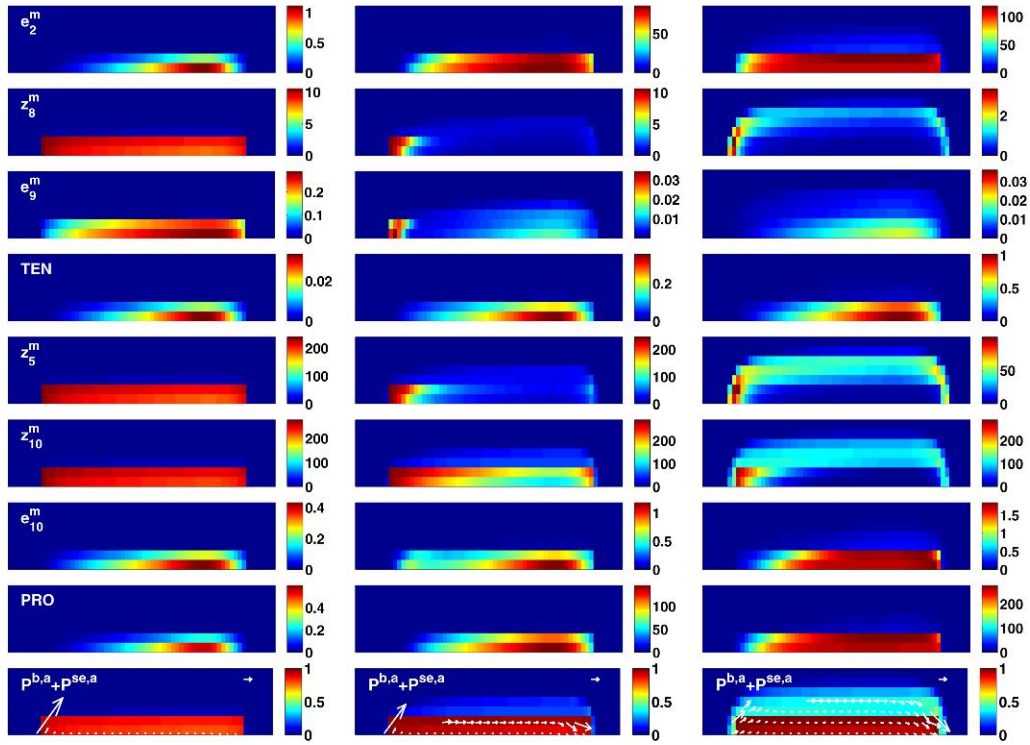

FIG. 12. Close-up of 120 μm long by 15 μm high region around thrombus at times 140, 180 and 250 s in left, middle and right columns, respectively. In each column are shown (top to bottom) spatial concentrations (nanomolar) of platelet-bound chemical species thrombin e_2^m, z_8^m, e_9^m and TEN (tenase) and z_5^m, z_{10}^m, e_{10}^m and PRO (prothrombinase) as well as the bound platelet concentration (fraction of P_{max}) and intrathrombus velocity (velocity scale vector 2 μm s^{-1}). The wall shear rate is 500 s^{-1}, the platelet profile is P_1 and the TF density is 15 fmol cm^{-2}.

sufficient to activate Z_8^m to E_8^m, which rapidly binds to E_9^m to form the tenase (TEN) complex. This happens only at the downstream end of the thrombus because that is where thrombin and E_9^m are found. Since the platelet-bound zymogen Z_{10}^m is also abundant there, the tenase complexes produce substantial platelet-bound Xa (E_{10}^m) in the downstream portion of the thrombus. In addition to activating Z_8^m to E_8^m, the thrombin in this portion of the thrombus activates Z_5^m to E_5^m, which together with the E_{10}^m produced by the tenase complexes, forms new prothrombinase complexes, which, in turn, produce more thrombin. Up to this time, factor Xa made at the subendothelial surface by TF:VIIa has been largely responsible for thrombin production; it has been the dominant activator of platelet-bound E_5^m, and it has combined with the E_5^m molecules to form prothrombinase. With the formation of substantial numbers of tenase complexes in the downstream portions of the thrombus, another powerful source of E_{10}^m comes into play, while thrombin takes over as the dominant activator of E_5^m.

By 180 s, both Xa and thrombin have diffused a small distance upstream, binding and unbinding from the bound platelet surfaces as they move. The thrombin activates almost all the platelet-bound zymogens Z_5^m and Z_8^m on the platelets it reaches, and the Xa binds to the platelets and forms prothrombinase complexes with the newly activated E_5^m. Thus, the availability of prothrombinase moves upstream through the thrombus as a consequence of upstream diffusion of thrombin and Xa from their downstream

sources against the weak flow then present in the thrombus. By time 250 s, the effect of diffusion is even more apparent. Tenase is still found predominantly at the downstream end of the thrombus, but both platelet-bound Xa and prothrombinase are found in the upstream portions of the thrombus.

4. Discussion

We have developed the first spatial–temporal model of platelet aggregation and blood coagulation under flow that includes detailed descriptions of coagulation biochemistry, chemical activation and deposition of blood platelets as well as the two-way interaction between the fluid dynamics and the growing platelet mass. Using this model, we were able to confirm prediction of a TF threshold made using a simpler model by Kuharsky & Fogelson (2001). We were able to understand the origin of this behaviour as well as explain why thrombin production plateaus at high levels of TF exposure. By looking at thrombus growth for different wall shear rates and platelet concentration profiles, we gained insight into how near-wall flow velocities and near-wall platelet concentrations contribute to the thrombus size and density in distinct ways. Two different chemical agonists are able to activate platelets in our model and we learned how each affects thrombus development during various stages of growth and spatial location. By accounting for the porosity of a developing thrombus, we explored how advective and diffusive transport within the thrombus affect growth of the thrombus in different ways, again with these affects varying with time and spatial location.

4.1 *Thrombin production dependence on TF density*

The level of exposure of TF is a critical determinant of the response of the coagulation system. About 1% of circulating factor VII is the active form factor VIIa. On its own, factor VIIa is a weak enzyme, but when bound to a subendothelial TF molecule, it becomes a powerful activator of factors IX and X. Presumably, small amounts of TF are routinely exposed to the blood by small injury or other means. Because of the threshold nature of the system's response to the level of TF exposure, these small amounts of TF do not trigger a substantial production of thrombin. Yet, if a more sizeable trauma causes a sufficiently high exposure of TF, the response of the system is rapid and strong.

Based on our simulations, we believe that the essential condition that has to achieved to trigger a substantial response is the 'simultaneous' availability of platelet-bound factor VIIIa and fluid-phase or platelet-bound factor IXa. These are the cofactor and enzyme components of the tenase complex that can form on the surface of activated platelets. Factor IXa is produced only by subendothelial TF:VIIa (in the model) and thus, its production depends on the density of TF:VIIa on the subenothelium and thus on the density of TF exposed. Because the progressing deposition of platelets on the subendothelium reduces and eventually eliminates the accessibility of TF:VIIa to its substrates, production of factor IXa is limited largely to the first 2 min following injury, and much of the IXa produced is carried away by flow or inhibited by the fluid-phase inhibitor ATIII. Removal by flow or inhibition by ATIII are also the fate of most of the factor Xa activated by TF:VIIa. Since this is the dominant activator of platelet-bound VIIIa during the first 60 s following injury, the density of TF:VIIa exposed also, indirectly, strongly influences the availability of factor VIIIa during the early stages of coagulation. Although we have not yet studied hemophilia with our new model, we note that hemophilias A and B are deficiencies in the plasma levels of factors VIII and IX, respectively. Without the activated forms of these factors (activated directly or indirectly by TF:VIIa as just described), the initial stimulus for coagulation is not successfully transferred to the surfaces of the depositing platelets.

Our model currently does not include factor XI and its activated form factor XIa. There is increasing experimental support for a possible role of XI in the coagulation process; it has been shown that thrombin can activate XI to XIa and that XIa can activate factor IX to IXa. This second pathway to factor IXa production is believed by some to be important in determining the ultimate levels of thrombin produced late in the coagulation process. Recent simulations based on an extension of the KF model (unpublished data) suggest that it is only at very low shear rates (10–100 s^{-1}) that this pathway significantly augments thrombin production. Yet, it will be interesting to extend the spatial–temporal model we present here to look at this as well.

The availability of surface-bound cofactor molecules (such as TF) and binding sites for cofactors, enzymes and substrates on the surfaces of activated platelets strongly influence coagulation events. Without these sites, the powerful enzyme complexes critical in coagulation would not form. The enzyme molecules generally compete for these sites with their zymogen precursors, and because the zymogen concentrations are typically larger than the corresponding enzyme concentrations, most binding sites are occupied by zymogen. For example, more than 90% of the platelet binding sites shared by factors IX and IXa is occupied by the zymogen. This is not the case, however, for the shared binding sites for factors X and Xa under conditions of high TF exposure. For a TF exposure of 15 fmol cm^{-2} or higher, formation of prothrombinase is limited because the great majority of these sites become occupied by Xa molecules that are part of the existing prothrombinase complexes. This implies that there are few or no empty binding sites for the precursor zymogen factor X, the substrate for tenase and consequently, the six-fold higher tenase concentration that forms for [TF] = 30 fmol cm^{-2} than at 15 fmol cm^{-2} does not lead to increased prothrombinase formation or thrombin production.

4.2 *Thrombus growth dependence on wall shear rate and near-wall excess of platelets*

In our simulations, if the platelet concentration is uniformly 250,000 platelets μL^{-1}, a typical plasma value, we see little thrombus growth beyond direct adhesion to the subendothelium. A three-fold increase in shear rate (from 500 to 1500 s^{-1}) and therefore in the rate at which platelets are brought to the vicinity of the injury does not lead to appreciable increases in platelet deposition at least for the value of the cohesion parameter k_{coh} used in these simulations (see below). By contrast, for nonuniform platelet concentration profiles similar to those measured experimentally, substantial thrombus growth occurs under the same conditions, which lead to little thrombus growth for the uniform profile.

Experimental data about the near-wall platelet excess are not clear about whether or to what extent the peak-to-centre concentration ratio increases with shear rate in the range 500–1500 s^{-1}. Hence, we looked at the effect of shear rate on thrombus growth both for a nonuniform profile that was the same for all shear rates and for a sequence of nonuniform profiles in which the peak-to-centre concentration itself increased with shear rate. The results for a fixed profile and increasing shear rate (Figs 7 and 8) show that changing the shear rate alone is not a factor in determining the overall size of the thrombus but that it does impact the size and distribution of high-density regions within the thrombus. Fig. 8f shows an increase in area of high density ($>90\%$) and the images in the second row of Fig. 7 show that new high-density regions develop in the more central portions of the thrombus as the shear rate increases. A possible explanation for this relies on the fact that, with increases in shear rate, both the delivery of platelets to the upstream end of the thrombus and their advection within the thrombus are higher. Thus, more platelets may enter the upstream end of the thrombus and be carried to its central portions before the density of bound platelets at the upstream end increases sufficiently to block further platelet transport through this portion of the thrombus.

As the near-wall platelet excess concentration becomes more pronounced, either because of changes of shear rate (Fig. 7, bottom row) or not (Fig. 7, right column), both the density of bound platelets within the thrombus and the overall size (area) of the thrombus increase. In both these sets of experiments, the advective flux of platelets to the injury increases. There is not, however, a simple relationship between the advective flux of platelets to the injury and the growth of the thrombus. This flux is the product of the local concentration of platelets and the local velocity of the fluid, so that the same flux results from different combinations of concentration and velocity that vary in inverse proportion to one another. Equal platelet fluxes do not necessarily imply equal thrombus growth. This is illustrated in Fig. 7(f and h). The ratio of the (initial) platelet flux in the simulation depicted in Fig. 7f to that depicted in Fig. 7h is about 6/5 (velocity ratio 3/2 and concentration ratio about 4/5); yet, the overall size of the thrombus and the size of the high-density region are greater in Fig. 7h.

The development and maintenance of an enhanced near-wall platelet concentration are the result of motion of red blood cells. Since we do not explicitly include red blood cells in our model, we instead prescribe the concentration profile for incoming platelets. For simulations in very long segments of a vessel, platelet diffusion would eventually cause the platelet profile to become close to uniform. This is not a serious issue in our simulations because the diffusion distance for the time it takes near-wall fluid to traverse the 240 μm long domain is only about 1 μm and so the profiles remain sharp throughout the domain.

4.3 *Platelet activation by chemical agonists*

Mobile unactivated platelets become activated by ADP or thrombin at rates that depend on the concentrations of these agonists. Once activated, mobile platelets can bind to platelets already part of the thrombus. It is on binding to the thrombus (or subendothelium) that a platelet becomes procoagulant (i.e. supports coagulation reactions on its surface) and its ADP secretion begins. While this may be a limitation in the model, it is not a serious one because activated platelets that remain unbound are rapidly carried downstream by the flow.

Prothrombinase, the enzyme complex that activates prothrombin to thrombin, is a platelet-bound complex. Therefore, thrombin production depends on the concentration of bound activated platelets. Since prothrombin is abundant in the plasma, thrombin production continues provided there are prothrombinase complexes available for prothrombin to bind.

ADP, by contrast, is nonrenewable in the sense that each platelet carries a finite amount of ADP that it can secrete into the plasma. Since fluid-phase ADP is rapidly removed by the flow, the concentration of ADP at a specific location depends largely on the ‘rate’ that platelets bind to the thrombus, not on the accumulated number of platelets already in the thrombus. Platelets rapidly adhere to the subendothelium during early thrombus development, so large amounts of ADP are secreted there and ADP-induced platelet activation is important during this period. The rate at which ADP-activated platelets bind to the thrombus peaks between 50 and 70 s at $\approx 5(10)^4$ platelets mm^{-3} s^{-1}), and this binding contributes to the early growth of the thrombus into the lumen. The initial burst of platelet activation by ADP is short lived because of ADP’s removal by flow and the slowing of platelet adhesion as coverage of the subendothelium progresses. The next burst of platelet activation, this time due to thrombin, between 150 and 240 s (see Fig. 9) leads to another round of ADP secretion and ADP-induced activation. Together, these lead to substantial growth of the thrombus. However, platelet activation by ADP and the binding of ADP-activated platelets to the thrombus have a relatively small affect on the overall thrombus size. This may be due in part to the relatively large activation threshold response (2 μm) of platelets to ADP used in the model simulations.

The spatial distribution of the agonist-induced platelet activation is also interesting. Initial deposition of platelets and hence ADP secretion and platelet activation are relatively uniform along the injury. Platelets activated near the downstream end of the injury have less opportunity to bind to the thrombus than those activated upstream because a substantial fraction of them is carried downstream (see Fig. 9). Later in the simulation, most of the chemical activation (by ADP and thrombin) occurs at the upstream end of the thrombus. A platelet activated there may bind there contributing to upstream growth or it may be carried into or over the thrombus binding downstream and contributing to upward growth of the thrombus or increased thrombus density.

4.4 *Transport in the thrombus*

To our knowledge, we have developed the first model of thrombus formation that considers the 'porous' nature of a growing platelet mass. Because a thrombus is porous, unactivated platelets and zymogens may be transported by flow into the thrombus and activated platelets and enzymes may be removed from its interior. The porosity of the thrombus is a model outcome; it evolves in space and time as a result of processes whose dynamics, themselves, depend on the porosity. Streamlines of the flow show that not all the fluid is diverted around the thrombus, but in fact flows directly through the interior. Platelets transported into the thrombus in this way may not be activated until they reach a chemical agonist far within the interior. As activated platelets are incorporated into parts of the thrombus, those parts become more dense and their permeability and the flow within them decrease, therefore restricting more flow or platelets from entering. This is apparent in the first 60 s when, because of platelet adhesion to the subendothelium, the near-wall velocity above the injury decreases from hundreds to less than one micron per second. By 2 min, the flow speed at the centre of the injury is at its minimum (see Fig. 10), and interestingly, this is precisely the time when thrombin begins to make a major appearance. The reduction in velocity aids in the sharp increase in thrombin production by allowing the enzymes, E_9 in particular, to remain within the thrombus for extended periods after their production. Moreover, our Peclet number studies revealed that diffusional transport was extremely important in upstream prothrombinase formation and thus thrombin production and further thrombus growth. The combined effects of increased contact times due to the reduction in velocity and diffusional transport of species upstream together cause substantial enhancement in the development of the thrombus.

4.5 *Flow boundary conditions*

In the simulations reported in this paper, we specify the velocity profile (hence the volumetric flow rate) at the inlet to the computational domain. In many laboratory experiments, a pump is used to impose a constant volumetric flux, so our simulations can be compared directly with such experiments. However, it is unclear whether these are the most appropriate flow boundary conditions for simulations of *in vivo* thrombus formation. It is inappropriate to drive the flow through the short vessel segment we simulate by imposing a constant pressure drop over that length that remains constant for the duration of the simulation. The reason is that as the thrombus grows, flow in the longer vessel, of which the computational domain is regarded to be a piece, slows and the pressure drop over the shorter segment actually increases. An alternative procedure is as follows: let the computational domain represent a small portion of a longer vessel over which the pressure drop is constant. In this case, we would indeed drive the flow with a pressure drop, but use a relationship (derived and used in Fogelson & Guy, 2004) between the flux and the pressure drop across just the computational domain while holding the pressure drop across the longer vessel fixed. We tried this method by running our simulation with a wall shear rate of 500 s^{-1},

a TF density of 15 fmol cm^{-2} and the platelet profile P_1. We used boundary conditions derived from this pressure–flow relationship and found that the results differed by less than 1% with the case of fixed inflow and Neumann outflow.

4.6 *Limitations and extensions*

Most of the model parameters have been previously estimated from the experimental literature (Kuharsky & Fogelson, 2001). Two new parameters about whose values we are less certain are the cohesion rate, k_{coh}, and the maximum resistance to flow within the thrombus, α_{max}. The parameter k_{coh} represents the rate of binding between two platelets already in relative positions that allow them to bind. We know of no comparable measurements in the literature. A fixed value of this parameter was used for all the simulations reported in this paper. In a limited set of simulations that used a 10-fold or 100-fold higher value of k_{coh}, there was surprisingly little change in thrombus area compared to what we describe here, but there was some change in the spatial structure of the platelet density distribution within the thrombus. The effects of using different values for k_{coh} warrants further study. It is also of interest to explore the model's behaviour if k_{coh} is made to depend on the local shear rate. In particular, this may change the linear rate of thrombus growth seen in Fig. 8(d–i).

In reference to α_{max}, which is the reciprocal of permeability, there are few measurements of thrombus permeability in the literature and none of these pertains to the permeability of a thrombus during its early stages of development. At times beyond those of interest in our simulations, the active process of 'clot retraction' pulls platelets into close proximity and squeezes out much of the fluid between the platelets. Hence, we expect 'old' thrombi to be much less porous than newly forming ones. One value for thrombus permeability we found in the literature is for thrombi extracted from abdominal aortic aneurysms. These develop over months and are therefore representative of old thrombi. The permeability reported for these thrombi is 0.91 ± 0.54 mm^4 N^{-1} s^{-1} (Adolph *et al.*, 1997); our minimum permeability is about six-fold larger than this, reflecting our belief that the early thrombus is much more porous than an old thrombus. We will explore further the effect of different levels of thrombus permeability in future simulations. It would be of immense help to have experimental measurements of the permeability of representative thrombi fixed at different relatively short times (e.g. 3, 5, 7 min) during their development.

We note that the current simulations do not include the effect of the inhibitor APC. APC is produced on the surfaces of endothelial cells by a complex of thrombin and endothelial-bound thrombomodulin. When we add endothelial reactions to the model (on surfaces upstream and downstream of the injury), APC production and its action of factors Va and VIIIa will be incorporated into the model. We do not expect this addition to profoundly change the results we report here because our earlier studies (Fogelson & Tania, 2005) with an extended KF model suggest that under flow situations, APC has little effect on events within the thrombus.

In this paper, we do not distinguish between the activation state of platelets activated in different ways. In reality, ADP, thrombin and subendothelial collagen elicit different subsets of the full range of platelet activation responses (Jennings, 2009). For example, ADP-activated platelets are not procoagulant without further stimulus, and there is some evidence that platelets activated by both collagen and thrombin are more procoagulant than platelets activated by either collagen or thrombin alone (Monroe & Hoffman, 2006). Assuming the latter is true, this would be another cause for spatial heterogeneity within a thrombus, as only platelets close to the injured wall could be activated by collagen. There is also increasing indication that unactivated platelets may be able to bind, if only transiently, to a growing thrombus (Jackson, 2007; Ruggeri & Mendolicchio, 2007). By increasing the time that a platelet is in

the vicinity of a developing thrombus, such binding would increase the platelet's time of exposure to chemical agonists and this would possibly lead to more activation and faster thrombus growth. All these features can be readily incorporated into extensions of our model and we will report on their consequences in future publications.

Acknowledgements

The authors would like to thank Robert Guy and James Keener for meaningful discussions. A grant of computer time from the Center for High Performance Computing at the University of Utah is gratefully acknowledged.

Funding

National Science Foundation (RTG DMS-0354259, DMS-0540779); National Institute of General Medical Sciences (R01-GM090203).

REFERENCES

ADOLPH, R., VORP, D. A., STEED, D. L., WEBSTER, M. W., KAMENEVA, M. V. & WATKINS, S. C. (1997) Cellular content and permeability of intraluminal thrombus in abdominal aortic aneurysm. *J. Vasc. Surg.*, **25**, 916–926.

AHMAD, S. S., RAWALA-SHEIKH, R. & WALSH, P. N. (1989) Comparative interactions of factor IX and factor IXa with human platelets. *J. Biol. Chem.*, **264**, 3244–3251.

ANAND, M., RAJAGOPAL, K. & RAJAGOPAL, K. (2003) A model incorporating some of the mechanical and biochemical factors underlying clot formation and dissolution in flowing blood. *J. Theor. Med.*, **5**, 183–218.

BELTRAMI, E. & JESTY, J. (2001) The role of membrane patch size and flow in regulating a proteolytic feedback threshold on a membrane: possible application in blood coagulation. *Math. Biosci.*, **172**, 1–13.

BODNAR, T. & SEQUEIRA, A. (2008) Numerical simulation of the coagulation dynamics of blood. *Comput. Math. Methods Med.*, **9**, 83–104.

BRASS, L. F., AHUJA, M., BELMONTE, E., PIZARRO, S., TARVER, A. & HOXIE, J. (1994) The human platelet thrombin receptor. Turning it on and turning it off. *Ann. N. Y. Acad. Sci.*, **714**, 1–12.

BUTENAS, S. & MANN, K. G. (1996) Kinetics of human factor VII activation. *Biochemistry*, **35**, 1904–1910.

ECKSTEIN, E. C. & BELGACEM, F. (1991) Model of platelet transport in flowing blood with drift and diffusion terms. *Biophys. J.*, **60**, 53–69.

ECKSTEIN, E. C., TILLES, A. W. & MILLERO III, F. J. (1988) Conditions for the occurrence of large near-wall excesses of small particles during blood flow. *Microvasc. Res.*, **36**, 31–39.

ERMAKOVA, E., PANTELEEV, M. & SHNOL, E. (2005) Blood coagulation and propagation of autowaves in flow. *Pathophysiol. Haemost. Thromb.*, **34**, 135–142.

FOGELSON, A. L. & GUY, R. D. (2004) Platelet-wall interactions in continuum models of platelet aggregation: formulation and numerical solution. *Math. Med. Biol.*, **21**, 293–334.

FOGELSON, A. L. & GUY, R. D. (2008) Immersed-boundary-type models of intravascular platelet aggregation. *Comput. Methods Appl. Mech. Eng.*, **197**, 2087–2104.

FOGELSON, A. L. & TANIA, N. (2005) Coagulation under flow: the influence of flow-mediated transport on the initiation and inhibition of coagulation. *Pathophysiol. Haemost. Thromb.*, **34**, 91–108.

GEAR, A. R. L. (1994) Platelet adhesion, shape change, and aggregation: rapid initiation and signal transduction events. *Can. J. Physiol. Pharmacol.*, **72**, 285–294.

GRABOWSKI, E., FRANTA, J. & DIDISHEIM, P. (1978) Platelet aggregation in flowing blood *in vitro* II. Dependence of aggregate growth rate on ADP concentration and shear rate. *Microvasc. Res.*, **16**, 183–195.

HATHCOCK, J. J. & NEMERSON, Y. (2004) Platelet deposition inhibits tissue factor activity: in vitro clots are impermeable to factor Xa. *Blood*, **104**, 123–127.

HEMKER, H. C. & KESSELS, H. (1991) Feedback mechanisms in coagulation. *Haemostasis*, **21**, 189–196.

HILL-EUBANKS, D. C. & LOLLAR, P. (1990) von Willibrand factor is a cofactor for thrombin-catalyzed cleavage of the Factor VIII light chain. *J. Biol. Chem.*, **265**, 17854–17858.

HOCKIN, M., JONES, K., EVERSE, S. & MANN, K. G. (2002) A model for the stoichiometric regulation of blood coagulation. *J. Biol. Chem.*, **277**, 18322–18333.

JACKSON, S. P. (2007) The growing complexity of platelet aggregation. *Blood*, **109**, 5087–5095.

JENNINGS, L. (2009) Mechanisms of platelet activation: need for new strategies to protect against platelet-mediated atherothrombosis. *Thromb. Haemost.*, **102**, 248–257.

JESTY, J. & NEMERSON, Y. (1995) The pathways of blood coagulation. *Williams Hematology* (E. Beutler, M. Lichtman & B. Coller eds), 5th edn. New York: McGraw-Hill, p. 1227–1238.

JESTY, J., WUN, T. & LORENZ, A. (1994) Kinetics of the inhibition of factor Xa and the tissue factor-factor VIIa complex by the tissue factor pathway inhibitor in the presence and absence of heparin. *Biochemistry*, **33**, 12686–12694.

JONES, K. & MANN, K. G. (1994) A model for the tissue factor pathway to thrombin. II. A mathematical simulation. *J. Biol. Chem.*, **269**, 23367–23373.

KRISHNASWAMY, S., JONES, K. C. & MANN, K. G. (1988) Prothrombinase complex assembly. Kinetic mechanism of enzyme assembly on phospholipid vesicles. *J. Biol. Chem.*, **263**, 3823–3834.

KUHARSKY, A. L. & FOGELSON, A. L. (2001) Surface-mediated control of blood coagulation: the role of binding site densities and platelet deposition. *Biophys. J.*, **80**, 1050–1074.

LEIDERMAN, K., MILLER, L. & FOGELSON, A. (2008) The effects of spatial inhomogeneities on flow through the endothelial surface layer. *J. Theor. Biol.*, **252**, 313–325.

LEVEQUE, R. J. (1996) High-resolution conservative algorithms for advection in incompressible flow. *SIAM J. Numer. Anal.*, **33**, 627–665.

LOBANOV, A. I. & STAROZHILOVA, T. K. (2005) The effect of convective flows on blood coagulation processes. *Pathophysiol. Haemost. Thromb.*, **34**, 121–134.

LOBANOVA, E., SHNOL, E. & ATHAULLAKHANOV, F. (2004) Complex dynamics of the formation of spatially localized standing structures in the vicinity of saddle-node bifurcations of waves in the reaction-diffusion model of blood clotting. *Phys. Rev. E*, **70**, 032903.

LOLLAR, P., KNUTSON, G. J. & FASS, D. N. (1985) Activation of porcine factor VIII:C by thrombin and factor Xa. *Biochemistry*, **24**, 8056–8064.

MANN, K. G. (1987) The assembly of blood clotting complexes on membranes. *Trends Biochem. Sci.*, **12**, 229–233.

MANN, K. G. (1994) Prothrombin and thrombin. *Hemostasis and Thrombosis: Basic Principles and Clinical Practice* (R. Colman, J. Hirsh, V. Marder & E. Salzman eds), 3d edn. Philadelphia, PA: J.B. Lippincott Company, p. 184–199.

MANN, K. G., BOVILL, E. G. & KRISHNASWAMY, S. (1991) Surface-dependent reactions in the propagation phase of blood coagulation. *Ann. N. Y. Acad. Sci.*, **614**, 63–75.

MANN, K. G., KRISHNASWAMY, S. & LAWSON, J. H. (1992) Surface-dependent hemostasis. *Semin. Hematol.*, **29**, 213–226.

MANN, K. G., NESHEIM, M. E., CHURCH, W. R., HALEY, P. & KRISHNASWAMY, S. (1990) Surface-dependent reactions of the vitamin K-dependent enzyme complexes. *Blood*, **76**, 1–16.

MONKOVIC, D. D. & TRACY, P. B. (1990a) Activation of human factor V by factor Xa and thrombin. *Biochemistry*, **29**, 1118.

MONKOVIC, D. D. & TRACY, P. B. (1990b) Functional characterization of human platelet-released factor V and its activation by factor Xa and thrombin. *J. Biol. Chem.*, **265**, 17132–17140.

MONROE, D. & HOFFMAN, M. (2006) What does it take to make a perfect clot? *Arterioscler. Thromb. Vasc. Biol.*, **26**, 41–48.

MORRISSEY, J. H. (1995) Tissue factor modulation of factor VIIa activity: use in measuring trace levels of factor VIIa in plasma. *Thromb. Haemost.*, **74**, 185–188.

NEMERSON, Y. (1992) The tissue factor pathway of blood coagulation. *Semin. Hematol.*, **29**, 170–176.

NESHEIM, M. E., PITTMAN, D. D., WANG, J. H., SLONOSKY, D., GILES, A. R. & KAUFMAN, R. J. (1988) The binding of s-labeled recombinant factor VIII to activated and unactivated human platelets. *J. Biol. Chem.*, **263**, 16467.

NESHEIM, M. E., TRACY, R. P., TRACY, P. B., BOSKOVIC, D. S. & MANN, K. G. (1992) Mathematical simulation of prothrominase. *Methods Enzymol.*, **215**, 316–328.

NOVOTNY, W. F., BROWN, S., MILETICH, J., RADER, D. & BROZE, G. (1991) Plasma antigen levels of the lipoprotein-associated coagulation inhibitor in patient samples. *Blood*, **78**, 387–393.

OKORIE, U., DENNEY, W. S., CHATTERJEE, M. S., NEEVES, K. B. & DIAMOND, S. L. (2008) Determination of surface tissue factor thresholds that trigger coagulation at venous and arterial shear rates: amplification of 100 fM circulating tissue factor requires flow. *Blood*, **111**, 3507–3513.

RAWALA-SHEIKH, R., AHMAD, S. S., ASHBY, B. & WALSH, P. N. (1990) Kinetics of coagulation factor X activation by platelet-bound factor IXa. *Biochemistry*, **29**, 2606–2611.

REED, G., FITZGERALD, M. & POLGAR, J. (2000) Molecular mechanisms of platelet exocytosis: insights into the secrete life of thrombocytes. *Blood*, **96**, 3334–3342.

ROSENBERG, R. & BAUER, K. (1994) The heparin-antithrombin system: a natural anticoagulant mechanism. *Hemostasis and Thrombosis: Basic Principles and Clinical Practice* (R. W. Colman, J. Hirsh, V. J. Marder & E. W. Salzman eds), 3d edn. Philadelphia, PA: J.B. Lippincott Company, p. 837–860.

RUGGERI, Z. & MENDOLICCHIO, C. (2007) Adhesion mechanics in platelet function. *Circ. Res.*, **100**, 1673–1685.

TANGELDER, G., TEIRLINCK, H., SLAAF, D. & RENEMAN, R. (1985) Distribution of blood platelets flowing in arterioles. *Am. J. Physiol.*, **248**, H318–H323.

TILLES, A. W. & ECKSTEIN, E. C. (1987) The near-wall excess of platelet-sized particles in blood flow: its dependence on hematocrit and wall shear rate. *Microvasc. Res.*, **33**, 211.

TURITTO, V. T. & BAUMGARTNER, H. R. (1979) Platelet interaction with subendothelium in flowing rabbit blood: effect of blood shear rate. *Microvasc. Res.*, **17**, 38–54.

TURITTO, V. T. & LEONARD, E. F. (1972) Platelet adhesion to a spinning surface. *Trans. Amer. Soc. Artif. Int. Organs*, **18**, 348–354.

TURITTO, V. T., WEISS, H. J. & BAUMGARTNER, H. R. (1980) The effect of shear rate on platelet interaction with subendothelium exposed to citrated human blood. *Microvasc. Res.*, **19**, 352–365.

TURITTO, V. T., WEISS, H. J., BAUMGARTNER, H. R., BADIMON, L. & FUSTER, V. (1987) Cells and aggregates at surfaces. *Ann. N. Y. Acad. Sci.*, 453–467.

WALSH, P. N. (1994) Platelet-coagulant protein interactions. *Hemostasis and Thrombosis: Basic Principles and Clinical Practice* (R. W. Colman, J. Hirsh, V. J. Marder & E. W. Salzman eds), 3d edn. Philadelphia, PA: J.B. Lippincott Company, p. 629–651.

WEISS, H. J. (1975) Platelet physiology and abnormalities of platelet function (Part 1). *New Engl. J. Med.*, **293**, 531–541.

XU, Z., CHEN, N., KAMOCKA, M., ROSEN, E. & ALBER, M. (2008) A multiscale model of thrombus development. *J. R. Soc. Interface*, **5**, 705–722.

XU, Z., CHEN, N., SHADDEN, S., MARSDEN, J., KAMOCKA, M., ROSEN, E. & ALBER, M. (2009) A multiscale model of thrombus development. *Soft Matter*, **5**, 769–779.

YEH, C., CALVEZ, A. & ECKSTEIN, E. (1994) An estimated shape function for drift in a platelet-transport model. *Biophys. J.*, **67**, 1252–1259.

YOUNG, M., CARROAD, P. & BELL, R. (1980) Estimation of diffusion coefficients of proteins. *Biotech. Bioeng.*, **22**, 947–955.

ZARNITSINA, V., ATAULLAKHANOV, F., LOBANOV, A. & MOROZOVA, O. (2001) Dynamics of spatially nonuniform patterning in the model of blood coagulation. *Chaos*, **11**, 57–70.

Appendix

A.1 *Notation*

Z_i and E_i refer to zymogen i and enzyme i in solution. Superscripts indicate membrane-bound versions of these proteins (e.g., E_7^{se}refers to the TF:VIIa complex and E_5^{m}refers to Factor Va bound to the platelet surface). Concentrations are denoted in a similar way but with lower-case z and e. Concentrations of binding sites on bound platelets for prothrombin/thrombin, factors V/Va, X/Xa, VIII/VIIIa, and IX/IXa are denoted: $N_i^b P^{b,a} + N_i^s P^{se,a}$, where N_2^b, N_5^b, N_{10}^b, N_8^b, and N_9^b refer to the number of binding sites for the zymogen-enzyme pairs expressed on the surface of a bound platelet (similar notation $N_i{}^s$ describes these quantities for a platelet bound directly to the subendothelium). A complex of Z_i and E_j is denoted $Z_i{:}E_j$ and its concentration is denoted $[Z_i{:}E_j]$. Special symbols are used for the platelet-bound 'tenase' VIIIa:IXa and 'prothrombinase' Va:Xa complexes, TEN = VIIIa:IXa and PRO = Va:Xa, and [TEN] and [PRO] denote their respective concentrations. The special symbol TFPIa is used for the fluid-phase complex TFPI:Xa, and [TFPIa] denotes its concentration. The inhibitors are denoted APC and $TFPI$ and their concentrations are denoted [APC] and [TFPI].

TABLE A1 *Diffusion coefficients for platelets and mobile chemical species*

Platelets	2.5×10^{-7} cm^2/s	Turitto & Leonard (1972)
ADP	5×10^{-6} cm^2/s	Grabowski *et al.* (1978)
All other chemical species	5×10^{-7} cm^2/s	Young *et al.* (1980)

TABLE A2 *Normal concentrations and surface binding site numbers*

Prothrombin	1.4 μM	Mann *et al.* (1990)
Factor V	0.01 μM	Mann *et al.* (1991)
Factor VII	0.01 μM	Mann *et al.* (1990)
Factor VIIa	0.1 nM	Morrissey (1995)
Factor VIII	1.0 nM	Mann *et al.* (1990)
Factor IX	0.09 μM	Mann *et al.* (1990)
Factor X	0.17 μM	Mann *et al.* (1990)
TFPI	2.5 nM	Novotny *et al.* (1991)
Platelets, P_0	2.5 $(10)^5$ mm^{-3}	Weiss (1975)
N_2^{b}, N_2^{se}	2000	Brass *et al.* (1994)
N_5^{b}, N_5^{se}	3000	Walsh (1994)
N_8^{b}, N_8^{se}	450	Nesheim *et al.* (1988)
N_9^{b}, N_9^{se}	500	Ahmad *et al.* (1989)
N_{10}^{b}, N_{10}^{se}	2700	Mann *et al.* (1992)

TABLE A3 *Reactions on subendothelium*

Reaction	Reactants	Complex	Product	$M^{-1}s^{-1}$	s^{-1}	s^{-1}	Note
Activation (of-, by-)							
(TF:VII, Xa)	E_{10}, Z_7^{se}	Z_7^{se}:E_{10}	E_7^{se}	$k^+_{z_7^{se}:e_{10}} = 5.0 \times 10^6$	$k^-_{z_7^{se}:e_{10}} = 1.0$	$k^{cat}_{z_7^{se}:e_{10}} = 5.0$	a
(TF:VII, IIa)	E_2, Z_7^{se}	Z_7^{se}:E_2	E_7^{se}	$k^+_{z_7^{se}:e_2} = 3.92 \times 10^5$	$k^-_{z_7^{se}:e_2} = 1.0$	$k^{cat}_{z_7^{se}:e_2} = 6.1 \times 10^{-2}$	b
(X, TF:VIIa)	E_7^{se}, Z_{10}	Z_{10}:E_7^{se}	E_{10}	$k^+_{z_{10}:e_7^{se}} = 8.95 \times 10^6$	$k^-_{z_{10}:e_7^{se}} = 1.0$	$k^{cat}_{z_{10}:e_7^{se}} = 1.15$	c
(IX, TF:VIIa)	E_7^{se}, Z_9	Z_9:E_7^{se}	E_9	$k^+_{z_9:e_7^{se}} = 8.95 \times 10^6$	$k^-_{z_9:e_7^{se}} = 1.0$	$k^{cat}_{z_9:e_7^{se}} = 1.15$	d
Binding (-, with -)							
(VII, TF)	Z_7, TF		Z_7^{se}	$k_7^{on} = 5.0 \times 10^7$	$k_7^{off} = 5.0 \times 10^{-3}$		e
(VIIa, TF)	E_7, TF		E_7^{se}	$k_7^{on} = 5.0 \times 10^7$	$k_7^{off} = 5.0 \times 10^{-3}$		e

a, $k^{cat}_{z_7^{se}:e_{10}} = 5.0\ s^{-1}$ and $K_M = 1.2 \times 10^{-6}$ M (Butenas & Mann, 1996);

b, $k^{cat}_{z_7^{se}:e_2} = 6.1 \times 10^{-2}\ s^{-1}$ and $K_M = 2.7 \times 10^{-6}$ M (Butenas & Mann, 1996);

c, $k^{cat}_{z_{10}:e_7^{se}} = 1.15\ s^{-1}$ and $K_M = 4.5 \times 10^{-7}$ M (Mann *et al.*, 1990);

d, We assume that the reaction constants for TF:VIIa activation of fIX are the same as for TF:VIIa activation of fX; e, $K_d = 1.0 \times 10^{-10}$ M (Nemerson, 1992).

TABLE A4 *Reactions in the plasma*

Reaction	Reactants	Complex	Product	$M^{-1}s^{-1}$	s^{-1}	s^{-1}	Note
Activation (of-, by-)							
(VII, Xa)	Z_7, E_{10}	Z_7:E_{10}	E_7	$k^+_{z_7:e_{10}} = 5 \times 10^6$	$k^-_{z_7:e_{10}} = 1.0$	$k^{cat}_{z_7:e_{10}} = 5.0$	a
(VII, IIa)	Z_7, E_2	Z_7:E_2	E_7	$k^+_{z_7:e_2} = 3.92 \times 10^5$	$k^-_{z_7:e_2} = 1.0$	$k^{cat}_{z_7:e_2} = 6.1 \times 10^{-2}$	b
(V, IIa)	Z_5, E_2	Z_5:E_2	E_5	$k^+_{z_5:e_2} = 1.73 \times 10^7$	$k^-_{z_5:e_2} = 1.0$	$k^{cat}_{z_5:e_2} = 0.23$	c
(VIII, IIa)	Z_8, E_2	Z_8:E_2	E_8	$k^+_{z_8:e_2} = 2.64 \times 10^7$	$k^-_{z_8:e_2} = 1.0$	$k^{cat}_{z_8:e_2} = 0.9$	d

a, $k^{cat}_{z_7:e_{10}} = 5.0\ s^{-1}$ and $K_M = 1.2 \times 10^{-6}$ M (Butenas & Mann, 1996);

b, $k^{cat}_{z_7:e_2} = 6.1 \times 10^{-2}\ s^{-1}$ and $K_M = 2.7 \times 10^{-6}$ M (Butenas & Mann, 1996);

c, $k^{cat}_{z_5:e_2} = 0.23\ s^{-1}$ and $K_M = 7.17 \times 10^{-8}$ M (Monkovic & Tracy, 1990b);

d, $k^{cat}_{z_8:e_2} = 0.9\ s^{-1}$ (Hill-Eubanks & Lollar, 1990) and $K_M = 2 \times 10^{-7}$ M (Lollar *et al.*, 1985).

TABLE A5 *Binding to platelet surfaces*

Reaction	Reactants	Products	$M^{-1}\ s^{-1}$	s^{-1}	Note
Factor IX	$Z_9,\ P_9$	Z_9^m	$k_9^{on} = 1.0 \times 10^7$	$k_9^{off} = 2.5 \times 10^{-2}$	a
Factor IXa	$E_9,\ P_9$	E_9^m	$k_9^{on} = 1.0 \times 10^7$	$k_9^{off} = 2.5 \times 10^{-2}$	a
Factor IXa	$E_9,\ P_9^*$	$E_9^{m,*}$	$k_9^{on} = 1.0 \times 10^7$	$k_9^{off} = 2.5 \times 10^{-2}$	b
Factor X	$Z_{10},\ P_{10}$	Z_{10}^m	$k_{10}^{on} = 1.0 \times 10^7$	$k_{10}^{off} = 2.5 \times 10^{-2}$	a
Factor Xa	$E_{10},\ P_{10}$	E_{10}^m	$k_{10}^{on} = 1.0 \times 10^7$	$k_{10}^{off} = 2.5 \times 10^{-2}$	a
Factor V	$Z_5,\ P_5$	Z_5^m	$k_5^{on} = 5.7 \times 10^7$	$k_5^{off} = 0.17$	c
Factor Va	$E_5,\ P_5$	E_5^m	$k_5^{on} = 5.7 \times 10^7$	$k_5^{off} = 0.17$	c
Factor VIII	$Z_8,\ P_8$	Z_8^m	$k_8^{on} = 5.0 \times 10^7$	$k_8^{off} = 0.17$	d
Factor VIIIa	$E_8,\ P_8$	E_8^m	$k_8^{on} = 5.0 \times 10^7$	$k_8^{off} = 0.17$	d
Factor II	$Z_2,\ P_2$	Z_2^m	$k_2^{on} = 1.0 \times 10^7$	$k_2^{off} = 5.9$	e
Factor IIa	$E_2,\ P_2$	E_2	$k_2^{on} = 1.0 \times 10^7$	$k_2^{off} = 5.9$	e

a, For fIX binding to platelets, $K_d = 2.5 \times 10^{-9}$ M (Ahmad *et al.*, 1989), and for fX binding to platelets, K_d has approximately the same value (Walsh, 1994). For fX binding to phospholipids (PCPS) vesicles, the on-rate is about $10^7\ M^{-1}\ s^{-1}$ and the off-rate is about $1.0\ s^{-1}$ (Krishnaswamy *et al.*, 1988), giving a dissociation constant of about 10^{-7} M. To estimate on- and off-rates for the higher-affinity binding of fX to platelets, we keep the on-rate the same as for vesicles and adjust the off-rate to give the correct dissociation constant. The rates for fIX binding with platelets are taken to be the same as for fX binding.

b, We assume binding constants for fIXa binding to the specific fIXa binding sites are the same as for shared sites.

c, The fV binds with high affinity to PCPS (Krishnaswamy *et al.*, 1988) and we use the same rate constants reported there to describe fV binding to platelets.

d, The K_d for fVIII binding with platelets is taken from (Nesheim *et al.*, 1988). We set the off-rate k_8^{off} for fVIII binding to platelets equal to that for fV binding to platelets and calculate the on-rate k_8^{on}.

e, For prothrombin interactions with platelets, K_d is reported to be 5.9×10^{-7} M (Mann, 1994). We choose k_2^{off} and set $k_2^{on} = k_2^{off}/K_d$.

TABLE A6 *Reactions on platelet surfaces*

Reaction	Reactants	Complex	Product	$M^{-1}\ s^{-1}$	s^{-1}	s^{-1}	Note
Activation (of-, by-)							
(V, Xa)	Z_5^m, E_{10}^m	Z_5^m:E_{10}^m	E_5^m	$k^+_{z_5^m:e_{10}^m} = 1.0 \times 10^8$	$k^-_{z_5^m:e_{10}^m} = 1.0$	$k^{cat}_{z_5^m:e_{10}^m} = 4.6 \times 10^{-2}$	a
(V, IIa)	Z_5^m, E_2^m	Z_5^m:E_2^m	E_5^m	$k^+_{z_5^m:e_2^m} = 1.73 \times 10^7$	$k^-_{z_5^m:e_2^m} = 1.0$	$k^{cat}_{z_5^m:e_2^m} = 0.23$	b
(VIII, Xa)	Z_8^m, E_{10}^m	Z_8^m:E_{10}^m	E_8^m	$k^+_{z_8^m:e_{10}^m} = 5.1 \times 10^7$	$k^-_{z_8^m:e_{10}^m} = 1.0$	$k^{cat}_{z_8^m:e_{10}^m} = 2.3 \times 10^{-2}$	c
(VIII, IIa)	Z_8^m, E_2^m	Z_8^m:E_2^m	E_8^m	$k^+_{z_8^m:e_2^m} = 2.64 \times 10^7$	$k^-_{z_8^m:e_2^m} = 1.0$	$k^{cat}_{z_8^m:e_2^m} = 0.9$	d
(X, VIIIa:IXa)	Z_{10}^m, TEN	Z_{10}^m:TEN	E_{10}^m	$k^+_{z_{10}^m:ten} = 1.31 \times 10^8$	$k^-_{z_{10}^m:ten} = 1.0$	$k^{cat}_{z_{10}^m:ten} = 20.0$	f
(X, VIIIa:IXa*)	Z_{10}^m, TEN*	Z_{10}^m:TEN*	E_{10}^m	$k^+_{z_{10}^m:ten} = 1.31 \times 10^8$	$k^-_{z_{10}^m:ten} = 1.0$	$k^{cat}_{z_{10}^m:ten} = 20.0$	f
(II, Va:Xa)	Z_2^m, PRO	Z_2^m:PRO	E_2^m	$k^+_{z_2^m:pro} = 1.03 \times 10^8$	$k^-_{z_2^m:pro} = 1.0$	$k^{cat}_{z_2^m:pro} = 30.0$	g
Binding (-, with -)							
(IIIa, IXa)	E_8^m, E_9^m		TEN	$k^+_{ten} = 1.0 \times 10^8$	$k^-_{ten} = 0.01$		e
(VIIIa, IXa*)	E_8^m, $E_9^{m,*}$		TEN*	$k^+_{ten} = 1.0 \times 10^8$	$k^-_{ten} = 0.01$		e
(Va, Xa)	E_5^m, E_{10}^m		PRO	$k^+_{pro} = 1.0 \times 10^8$	$k^-_{pro} = 0.01$		e

a, $k^{cat}_{z_5^m:e_{10}^m} = 0.046\ s^{-1}$ and $K_M = 10.4 \times 10^{-9}$ M (Monkovic & Tracy, 1990a).
b, The rate constants for thrombin activation of fV on platelets are assumed to be the same as in plasma.
c, $k^{cat}_{z_8^m:e_{10}^m} = 0.023\ s^{-1}$ and $K_M = 2.0 \times 10^{-8}$ M (Lollar *et al.*, 1985).
d, The rate constants for thrombin activation of fVIII on platelets are assumed to be the same as in plasma.
e, The formation of the tenase and prothrombinase complexes is assumed to be very fast with $K_d = 1.0 \times 10^{-10}$ M (Mann, 1987).
f, $k^{cat}_{z_{10}^m:ten} = 20\ s^{-1}$ and $K_M = 1.6 \times 10^{-7}$ M (Rawala-Sheikh *et al.*, 1990).
g, $k^{cat}_{z_2^m:pro} = 30\ s^{-1}$ and $K_M = 3.0 \times 10^{-7}$ M (Nesheim *et al.*, 1992).

TABLE A7 *Inhibition reactions*

Reaction	Reactants	Product	$M^{-1}s^{-1}$	s^{-1}	Note
Inactivation (of-, by-)					
(IXa, ATIII)	E_9	$E_9{}^{,\mathrm{in}}$		$k_9^{\mathrm{in}} = 0.1$	a
(Xa, ATIII)	E_{10}	$E_{10}{}^{,\mathrm{in}}$		$k_{10}^{\mathrm{in}} = 0.1$	a
(IIa, ATIII)	E_2	$E_2{}^{,\mathrm{in}}$		$k_2^{\mathrm{in}} = 0.2$	a
Binding (-, with-)					
(TFPI, Xa)	TFPI, E_{10}	TFPIa	$k^+_{tfpia:e_{10}} = 1.6 \times 10^7$	$k^-_{tfpia:e_{10}} = 3.3 \times 10^{-4}$	b
(TFPIa, TF:VIIa)	TFPIa, E_7^{se}	TFPIa:E_7^{se}	$k^+_{tfpia:e_7^{se}} = 1.0 \times 10^7$	$k^-_{tfpia:e_7^{se}} = 1.1 \times 10^{-3}$	b

a, We estimate these parameters based on the half-lives of factors IXa, Xa and IIa in plasma (Rosenberg & Bauer, 1994).
b, Jesty *et al.* (1994). APC is not included in these simulations.

TABLE A8 *Platelet transitions*

Transition	Initial state	Final state	$M^{-1}\,s^{-1}$	s^{-1}	Note
Unactivated platelet adhering to SE	$P^{\mathrm{m,u}}$	$P^{\mathrm{se,a}}$	$k_{\mathrm{adh}} = 2 \times 10^{10}$		a
Bound platelet adhering to SE	$P^{\mathrm{b,a}}$	$P^{\mathrm{se,a}}$	$k_{\mathrm{adh}} = 2 \times 10^{10}$		a
Activated platelet adhering to SE	$P^{\mathrm{m,u}}$	$P^{\mathrm{se,a}}$	$k_{\mathrm{adh}} = 2 \times 10^{10}$		a
Activated platelet cohering to bound platelet	$P^{\mathrm{m,a}}$	$P^{\mathrm{b,a}}$		$k_{\mathrm{coh}} \times P_{\max} = 1 \times 10^4$	
Platelet activation by ADP	$P^{\mathrm{m,u}}$	$P^{\mathrm{m,a}}$		$k_{\mathrm{adp}}^{\mathrm{pla}} = 0.34$	b
Platelet activation by thrombin	$P^{\mathrm{m,u}}$	$P^{\mathrm{m,a}}$		$k_{e_2}^{\mathrm{pla}} = 0.50$	b

a, Estimated from data in Turitto & Baumgartner (1979) and Turitto *et al.* (1980) as described in Kuharsky & Fogelson (2001). SE means subendothelium.
b, Estimated from data in Gear (1994) as described in text.

A.2 *Model equations for chemicals*

A.2.1 *Subendothelium bound*

$$\begin{aligned}\frac{\partial z_7^{\mathrm{se}}}{\partial t} &= k_7^{\mathrm{on}} z_7([\mathrm{TF}] - e_7^{\mathrm{setot}} - z_7^{\mathrm{setot}}) - k_7^{\mathrm{off}} z_7^{\mathrm{se}} - k^+_{z_7^{se}:e_{10}} z_7^{\mathrm{se}} e_{10} \\ &\quad + k^-_{z_7^{se}:e_{10}}[Z_7^{\mathrm{se}}{:}E_{10}] - k^+_{z_7^{se}:e_2} z_7^{\mathrm{se}} e_2 + k^-_{z_7^{se}:e_2} k^+_{z_7^{se}:e_2}[Z_7^{\mathrm{se}}{:}E_2] \\ &\quad - k_{\mathrm{adh}}(\mathbf{x}) z_7^{\mathrm{se}}(P^{\mathrm{m,a}} + P^{\mathrm{m,u}} + P^{\mathrm{b,a}}), \end{aligned} \tag{A.1}$$

$$\begin{aligned}\frac{\partial e_7^{\mathrm{se}}}{\partial t} &= k_7^{\mathrm{on}} e_7([\mathrm{TF}] - e_7^{\mathrm{setot}} - z_7^{\mathrm{setot}}) - k_7^{\mathrm{off}} e_7^{\mathrm{se}} + k^{\mathrm{cat}}_{z_7^{se}:e_{10}}[Z_7^{\mathrm{se}}{:}E_{10}] \\ &\quad + k^{\mathrm{cat}}_{z_7^{se}:e_2}[Z_7^{\mathrm{se}}{:}E_2] + (k^-_{z_{10}:e_7^{se}} + k^{\mathrm{cat}}_{z_{10}:e_7^{se}})[Z_{10}{:}E_7^{\mathrm{se}}] \end{aligned}$$

$$
\begin{aligned}
&- k^{+}_{z_{10}:e_7^{se}} z_{10} e_7^{\mathrm{se}} + (k^{-}_{z_9:e_7^{se}} + k^{\mathrm{cat}}_{z_9:e_7^{se}})[Z_9{:}E_7^{\mathrm{se}}] - k^{+}_{z_9:e_7^{se}} z_9 e_7^{\mathrm{se}} \\
&- k^{+}_{tfpia:e_7^{se}}[\mathrm{TFPIa}] e_7^{\mathrm{se}} + k^{-}_{tfpia:e_7^{se}}[\mathrm{TFPIa}{:}E_7^{\mathrm{se}}] \\
&- k_{\mathrm{adh}}(\mathbf{x}) e_7^{\mathrm{se}} (P^{\mathrm{m,a}} + P^{\mathrm{m,u}} + P^{\mathrm{b,a}}), \qquad \text{(A.2)}
\end{aligned}
$$

$$
\begin{aligned}
\frac{\partial [Z_7^{\mathrm{se}}{:}E_2]}{\partial t} &= k^{+}_{z_7^{se}:e_2} z_7^{\mathrm{se}} e_2 - (k^{-}_{z_7^{se}:e_2} + k^{\mathrm{cat}}_{z_7^{se}:e_2})[Z_7^{\mathrm{se}}{:}E_2] \\
&- k_{\mathrm{adh}}(\mathbf{x})[Z_7^{\mathrm{se}}{:}E_2](P^{\mathrm{m,a}} + P^{\mathrm{m,u}} + P^{\mathrm{b,a}}), \qquad \text{(A.3)}
\end{aligned}
$$

$$
\begin{aligned}
\frac{\partial [Z_7^{\mathrm{se}}{:}E_{10}]}{\partial t} &= k^{+}_{z_7^{se}:e_{10}} z_7^{\mathrm{se}} e_{10} - (k^{-}_{z_7^{se}:e_{10}} + k^{\mathrm{cat}}_{z_7^{se}:e_{10}})[Z_7^{\mathrm{se}}{:}E_{10}] \\
&- k_{\mathrm{adh}}(\mathbf{x})[Z_7^{\mathrm{se}}{:}E_{10}](P^{\mathrm{m,a}} + P^{\mathrm{m,u}} + P^{\mathrm{b,a}}), \qquad \text{(A.4)}
\end{aligned}
$$

$$
\begin{aligned}
\frac{\partial [Z_9{:}E_7^{\mathrm{se}}]}{\partial t} &= k^{+}_{z_9:e_7^{se}} z_9 e_7^{\mathrm{se}} - (k^{-}_{z_9:e_7^{se}} + k^{\mathrm{cat}}_{z_9:e_7^{se}})[Z_9{:}E_7^{\mathrm{se}}] \\
&- k_{\mathrm{adh}}(\mathbf{x})[Z_9{:}E_7^{\mathrm{se}}](P^{\mathrm{m,a}} + P^{\mathrm{m,u}} + P^{\mathrm{b,a}}), \qquad \text{(A.5)}
\end{aligned}
$$

$$
\begin{aligned}
\frac{\partial [Z_{10}{:}E_7^{\mathrm{se}}]}{\partial t} &= k^{+}_{z_{10}:e_7^{se}} z_{10} e_7^{\mathrm{se}} - (k^{-}_{z_{10}:e_7^{se}} + k^{\mathrm{cat}}_{z_{10}:e_7^{se}})[Z_{10}{:}E_7^{\mathrm{se}}] \\
&- k_{\mathrm{adh}}(\mathbf{x})[Z_{10}{:}E_7^{\mathrm{se}}](P^{\mathrm{m,a}} + P^{\mathrm{m,u}} + P^{\mathrm{b,a}}), \qquad \text{(A.6)}
\end{aligned}
$$

$$
\begin{aligned}
\frac{\partial [\mathrm{TFPIa}{:}E_7^{\mathrm{se}}]}{\partial t} &= -k^{-}_{tfpia:e_7^{se}}[\mathrm{TFPIa}{:}E_7^{\mathrm{se}}] + k^{+}_{tfpia:e_7^{se}}[\mathrm{TFPIa}] e_7^{\mathrm{se}} \\
&- k_{\mathrm{adh}}(\mathbf{x})[\mathrm{TFPIa}{:}E_7^{\mathrm{se}}](P^{\mathrm{m,a}} + P^{\mathrm{m,u}} + P^{\mathrm{b,a}}), \qquad \text{(A.7)}
\end{aligned}
$$

$$
\frac{\partial [\mathrm{TF}]}{\partial t} = -k_{\mathrm{adh}}(\mathbf{x})[\mathrm{TF}](P^{\mathrm{m,a}} + P^{\mathrm{m,u}} + P^{\mathrm{b,a}}). \qquad \text{(A.8)}
$$

A.2.2 *Platelet bound*

$$
\begin{aligned}
\frac{\partial z_2^{\mathrm{m}}}{\partial t} &= k_2^{\mathrm{on}} z_2 (N_2^{\mathrm{b}} P^{\mathrm{b,a}} + N_2^{\mathrm{se}} P^{\mathrm{se,a}} - z_2^{\mathrm{mtot}} - e_2^{\mathrm{mtot}}) - k_2^{\mathrm{off}} z_2^{\mathrm{m}} \\
&- k^{+}_{z_2^m:pro} z_2^{\mathrm{m}}[\mathrm{PRO}] + k^{-}_{z_2^m:pro}[Z_2^{\mathrm{m}}{:}\mathrm{PRO}], \qquad \text{(A.9)}
\end{aligned}
$$

$$
\begin{aligned}
\frac{\partial e_2^{\mathrm{m}}}{\partial t} &= k_2^{\mathrm{on}} e_2 (N_2^{\mathrm{b}} P^{\mathrm{b,a}} + N_2^{\mathrm{se}} P^{\mathrm{se,a}} - z_2^{\mathrm{mtot}} - e_2^{\mathrm{mtot}}) \\
&- k_2^{\mathrm{off}} e_2^{\mathrm{m}} + k^{\mathrm{cat}}_{z_2^m:pro}[Z_2^{\mathrm{m}}{:}\mathrm{PRO}] \\
&+ (k^{\mathrm{cat}}_{z_5^m:e_2^m} + k^{-}_{z_5^m:e_2^m})[Z_5^{\mathrm{m}}{:}E_2^{\mathrm{m}}] - k^{+}_{z_5^m:e_2^m} z_5^{\mathrm{m}} e_2^{\mathrm{m}} \\
&+ (k^{\mathrm{cat}}_{z_8^m:e_2^m} + k^{-}_{z_8^m:e_2^m})[Z_8^{\mathrm{m}}{:}E_2^{\mathrm{m}}] - k^{+}_{z_8^m:e_2^m} z_8^{\mathrm{m}} e_2^{\mathrm{m}}, \qquad \text{(A.10)}
\end{aligned}
$$

$$\frac{\partial z_5^{\mathrm{m}}}{\partial t} = k_5^{\mathrm{on}} z_5 (N_5^{\mathrm{b}} P^{\mathrm{b,a}} + N_5^{\mathrm{se}} P^{\mathrm{se,a}} - z_5^{\mathrm{mtot}} - e_5^{\mathrm{mtot}}) - k_5^{\mathrm{off}} z_5^{\mathrm{m}}$$
$$- k^{+}_{z_5^m:e_{10}^m} z_5^{\mathrm{m}} e_{10}^{\mathrm{m}} + k^{-}_{z_5^m:e_{10}^m} [Z_5^{\mathrm{m}}{:}E_{10}^{\mathrm{m}}]$$
$$- k^{+}_{z_5^m:e_2^m} z_5^{\mathrm{m}} e_2^{\mathrm{m}} + k^{-}_{z_5^m:e_2^m} [Z_5^{\mathrm{m}}{:}E_2^{\mathrm{m}}], \tag{A.11}$$

$$\frac{\partial e_5^{\mathrm{m}}}{\partial t} = k_5^{\mathrm{on}} e_5 (N_5^{\mathrm{b}} P^{\mathrm{b,a}} + N_5^{\mathrm{se}} P^{\mathrm{se,a}} - z_5^{\mathrm{mtot}} - e_5^{\mathrm{mtot}}) - k_5^{\mathrm{off}} e_5^{\mathrm{m}} \tag{A.12}$$
$$+ k^{\mathrm{cat}}_{z_5^m:e_{10}^m} [Z_5^{\mathrm{m}}{:}E_{10}^{\mathrm{m}}] + k^{\mathrm{cat}}_{z_5^m:e_2^m} [Z_5^{\mathrm{m}}{:}E_2^{\mathrm{m}}] + k^{-}_{\mathrm{pro}} [\mathrm{PRO}]$$
$$- k^{+}_{\mathrm{pro}} e_5^{\mathrm{m}} e_{10}^{\mathrm{m}} - k^{+}_{apc:e_5^m} [\mathrm{APC}] e_5^{\mathrm{m}} + k^{-}_{apc:e_5^m} [\mathrm{APC}{:}E_5^{\mathrm{m}}],$$

$$\frac{\partial z_8^{\mathrm{m}}}{\partial t} = k_8^{\mathrm{on}} z_8 (N_8^{\mathrm{b}} P^{\mathrm{b,a}} + N_8^{\mathrm{se}} P^{\mathrm{se,a}} p_8^{\mathrm{m}} - z_8^{\mathrm{mtot}} - e_8^{\mathrm{mtot}}) - k_8^{\mathrm{off}} z_8^{\mathrm{m}}$$
$$- k^{+}_{z_8^m:e_{10}^m} z_8^{\mathrm{m}} e_{10}^{\mathrm{m}} + k^{-}_{z_8^m:e_{10}^m} [Z_8^{\mathrm{m}}{:}E_{10}^{\mathrm{m}}]$$
$$- k^{+}_{z_8^m:e_2^m} z_8^{\mathrm{m}} e_2^{\mathrm{m}} + k^{-}_{z_8^m:e_2^m} [Z_8^{\mathrm{m}}{:}E_2^{\mathrm{m}}], \tag{A.13}$$

$$\frac{\partial e_8^{\mathrm{m}}}{\partial t} = k_8^{\mathrm{on}} e_8 (N_8^{\mathrm{b}} P^{\mathrm{b,a}} + N_8^{\mathrm{se}} P^{\mathrm{se,a}} - z_8^{\mathrm{mtot}} - e_8^{\mathrm{mtot}}) - k_8^{\mathrm{off}} e_8^{\mathrm{m}}$$
$$+ k^{\mathrm{cat}}_{z_8^m:e_{10}^m} [Z_8^{\mathrm{m}}{:}E_{10}^{\mathrm{m}}] + k^{\mathrm{cat}}_{z_8^m:e_2^m} [Z_8^{\mathrm{m}}{:}E_2^{\mathrm{m}}] + k^{-}_{\mathrm{ten}} [\mathrm{TEN}]$$
$$- k^{+}_{\mathrm{ten}} e_8^{\mathrm{m}} e_9^{\mathrm{m}} - k^{+}_{apc:e_8^m} [\mathrm{APC}] e_8^{\mathrm{m}} + k^{-}_{apc:e_8^m} [\mathrm{APC}{:}E_8^{\mathrm{m}}], \tag{A.14}$$

$$\frac{\partial z_9^{\mathrm{m}}}{\partial t} = k_9^{\mathrm{on}} z_9 (N_9^{\mathrm{b}} P^{\mathrm{b,a}} + N_9^{\mathrm{se}} P^{\mathrm{se,a}} - z_9^{\mathrm{mtot}} - e_9^{\mathrm{mtot}}) - k_9^{\mathrm{off}} z_9^{\mathrm{m}}, \tag{A.15}$$

$$\frac{\partial e_9^{\mathrm{m}}}{\partial t} = k_9^{\mathrm{on}} e_9 (N_9^{\mathrm{b}} P^{\mathrm{b,a}} + N_9^{\mathrm{se}} P^{\mathrm{se,a}} - z_9^{\mathrm{mtot}} - e_9^{\mathrm{mtot}}) - k_9^{\mathrm{off}} e_9^{\mathrm{m}}$$
$$+ k^{-}_{\mathrm{ten}} [\mathrm{TEN}] - k^{+}_{\mathrm{ten}} e_8^{\mathrm{m}} e_9^{\mathrm{m}}, \tag{A.16}$$

$$\frac{\partial z_{10}^{\mathrm{m}}}{\partial t} = k_{10}^{\mathrm{on}} z_{10} (N_{10}^{\mathrm{b}} P^{\mathrm{b,a}} + N_{10}^{\mathrm{se}} P^{\mathrm{se,a}} - e_{10}^{\mathrm{mtot}} - z_{10}^{\mathrm{mtot}}) - k_{10}^{\mathrm{off}} z_{10}^{\mathrm{m}}$$
$$+ k^{-}_{z_{10}^m:ten} [Z_{10}^{\mathrm{m}}{:}\mathrm{TEN}] - k^{+}_{z_{10}^m:ten} z_{10}^{\mathrm{m}} [\mathrm{TEN}]$$
$$+ k^{-}_{z_{10}^m:ten} [Z_{10}^{\mathrm{m}}{:}\mathrm{TEN}^*] - k^{+}_{z_{10}^m:ten} z_{10}^{\mathrm{m}} [\mathrm{TEN}^*], \tag{A.17}$$

$$\frac{\partial e_{10}^{\mathrm{m}}}{\partial t} = k_{10}^{\mathrm{on}} e_{10} (N_{10}^{\mathrm{b}} P^{\mathrm{b,a}} + N_{10}^{\mathrm{se}} P^{\mathrm{se,a}} - e_{10}^{\mathrm{mtot}} - z_{10}^{\mathrm{mtot}}) - k_{10}^{\mathrm{off}} e_{10}^{\mathrm{m}}$$
$$+ (k^{-}_{z_5^m:e_{10}^m} + k^{\mathrm{cat}}_{z_5^m:e_{10}^m}) [Z_5^{\mathrm{m}}{:}E_{10}^{\mathrm{m}}] - k^{+}_{z_5^m:e_{10}^m} z_5^{\mathrm{m}} e_{10}^{\mathrm{m}}$$
$$+ (k^{-}_{z_8^m:e_{10}^m} + k^{\mathrm{cat}}_{z_8^m:e_{10}^m}) [Z_8^{\mathrm{m}}{:}E_{10}^{\mathrm{m}}] - k^{+}_{z_8^m:e_{10}^m} z_8^{\mathrm{m}} e_{10}^{\mathrm{m}}$$

$$+ k^{-}_{\mathrm{pro}}[\mathrm{PRO}] - k^{+}_{\mathrm{pro}} e^{\mathrm{m}}_{5} e^{\mathrm{m}}_{10} + k^{\mathrm{cat}}_{z^{m}_{10}:ten}[Z^{\mathrm{m}}_{10}{:}\mathrm{TEN}]$$

$$+ k^{\mathrm{cat}}_{z^{m}_{10}:ten}[Z^{\mathrm{m}}_{10}{:}\mathrm{TEN}^{*}], \tag{A.18}$$

$$\frac{\partial[\mathrm{TEN}]}{\partial t} = k^{+}_{\mathrm{ten}} e^{\mathrm{m}}_{8} e^{\mathrm{m}}_{9} - k^{-}_{\mathrm{ten}}[\mathrm{TEN}] - k^{+}_{z^{m}_{10}:ten} z^{\mathrm{m}}_{10}[\mathrm{TEN}]$$

$$+ (k^{\mathrm{cat}}_{z^{m}_{10}:ten} + k^{-}_{z^{m}_{10}:ten})[Z^{\mathrm{m}}_{10}{:}\mathrm{TEN}], \tag{A.19}$$

$$\frac{\partial[\mathrm{PRO}]}{\partial t} = k^{+}_{\mathrm{pro}} e^{\mathrm{m}}_{5} e^{\mathrm{m}}_{10} - k^{-}_{\mathrm{pro}}[\mathrm{PRO}] - k^{+}_{z^{m}_{2}:pro} z^{\mathrm{m}}_{2}[\mathrm{PRO}]$$

$$+ (k^{\mathrm{cat}}_{z^{m}_{2}:pro} + k^{-}_{z^{m}_{2}:pro})[Z^{\mathrm{m}}_{2}{:}\mathrm{PRO}], \tag{A.20}$$

$$\frac{\partial[Z^{\mathrm{m}}_{2}{:}\mathrm{PRO}]}{\partial t} = k^{+}_{z^{m}_{2}:pro} z^{\mathrm{m}}_{2}[\mathrm{PRO}] - (k^{-}_{z^{m}_{2}:pro} + k^{\mathrm{cat}}_{z^{m}_{2}:pro})[Z^{\mathrm{m}}_{2}{:}\mathrm{PRO}], \tag{A.21}$$

$$\frac{\partial[Z^{\mathrm{m}}_{5}{:}E^{\mathrm{m}}_{2}]}{\partial t} = k^{+}_{z^{m}_{5}:e^{m}_{2}} z^{\mathrm{m}}_{5} e^{\mathrm{m}}_{2} - (k^{-}_{z^{m}_{5}:e^{m}_{2}} + k^{\mathrm{cat}}_{z^{m}_{5}:e^{m}_{2}})[Z^{\mathrm{m}}_{5}{:}E^{\mathrm{m}}_{2}], \tag{A.22}$$

$$\frac{\partial[Z^{\mathrm{m}}_{5}{:}E^{\mathrm{m}}_{10}]}{\partial t} = k^{+}_{z^{m}_{5}:e^{m}_{10}} z^{\mathrm{m}}_{5} e^{\mathrm{m}}_{10} - (k^{-}_{z^{m}_{5}:e^{m}_{10}} + k^{\mathrm{cat}}_{z^{m}_{5}:e^{m}_{10}})[Z^{\mathrm{m}}_{5}{:}E^{\mathrm{m}}_{10}], \tag{A.23}$$

$$\frac{\partial[Z^{\mathrm{m}}_{8}{:}E^{\mathrm{m}}_{2}]}{\partial t} = k^{+}_{z^{m}_{8}:e^{m}_{2}} z^{\mathrm{m}}_{8} e^{\mathrm{m}}_{2} - (k^{-}_{z^{m}_{8}:e^{m}_{2}} + k^{\mathrm{cat}}_{z^{m}_{8}:e^{m}_{2}})[Z^{\mathrm{m}}_{8}{:}E^{\mathrm{m}}_{2}], \tag{A.24}$$

$$\frac{\partial[Z^{\mathrm{m}}_{8}{:}E^{\mathrm{m}}_{10}]}{\partial t} = k^{+}_{z^{m}_{8}:e^{m}_{10}} z^{\mathrm{m}}_{8} e^{\mathrm{m}}_{10} - (k^{-}_{z^{m}_{8}:e^{m}_{10}} + k^{\mathrm{cat}}_{z^{m}_{8}:e^{m}_{10}})[Z^{\mathrm{m}}_{8}{:}E^{\mathrm{m}}_{10}], \tag{A.25}$$

$$\frac{\partial[Z^{\mathrm{m}}_{10}{:}\mathrm{TEN}]}{\partial t} = k^{+}_{z^{m}_{10}:ten} z^{\mathrm{m}}_{10}[\mathrm{TEN}] - (k^{-}_{z^{m}_{10}:ten} + k^{\mathrm{cat}}_{z^{m}_{10}:ten})[Z^{\mathrm{m}}_{10}{:}\mathrm{TEN}], \tag{A.26}$$

$$\frac{\partial[\mathrm{APC}{:}E^{\mathrm{m}}_{5}]}{\partial t} = k^{+}_{apc:e^{m}_{5}}[\mathrm{APC}] e^{\mathrm{m}}_{5} - (k^{-}_{apc:e^{m}_{5}} + k^{\mathrm{cat}}_{apc:e^{m}_{5}})[\mathrm{APC}{:}E^{\mathrm{m}}_{5}], \tag{A.27}$$

$$\frac{\partial[\mathrm{APC}{:}E^{\mathrm{m}}_{8}]}{\partial t} = k^{+}_{apc:e^{m}_{8}}[\mathrm{APC}] e^{\mathrm{m}}_{8} - (k^{-}_{apc:e^{m}_{8}} + k^{\mathrm{cat}}_{apc:e^{m}_{8}})[\mathrm{APC}{:}E^{\mathrm{m}}_{8}], \tag{A.28}$$

$$\frac{\partial e^{\mathrm{m},*}_{9}}{\partial t} = k^{\mathrm{on}}_{9} e^{\mathrm{m}}_{9} (N^{\mathrm{b}}_{9*} P^{\mathrm{b,a}} + N^{\mathrm{se}}_{9*} P^{\mathrm{se,a}} - e^{\mathrm{m},*}_{9} - [\mathrm{TEN}^{*}] - [Z^{\mathrm{m}}_{10} : \mathrm{TEN}^{*}])$$

$$- k^{\mathrm{off}}_{9} e^{\mathrm{m},*}_{9} + k^{-}_{\mathrm{ten}}[\mathrm{TEN}^{*}] - k^{+}_{\mathrm{ten}} e^{\mathrm{ten}}_{8} e^{\mathrm{m},*}_{9}, \tag{A.29}$$

$$\frac{\partial[\mathrm{TEN}^{*}]}{\partial t} = k^{+}_{\mathrm{ten}} e^{\mathrm{m}}_{8} e^{\mathrm{m},*}_{9} - k^{-}_{\mathrm{ten}}[\mathrm{TEN}^{*}]$$

$$+ (k^{-}_{z^{m}_{10}:ten} + k^{\mathrm{cat}}_{z^{m}_{10}:ten})[Z^{\mathrm{m}}_{10}{:}\mathrm{TEN}^{*}] - k^{+}_{z^{m}_{10}:ten} z^{\mathrm{m}}_{10}[\mathrm{TEN}^{*}], \tag{A.30}$$

$$\frac{\partial[Z_{10}^{\mathrm{m}}{:}\mathrm{TEN}^*]}{\partial t} = k^+_{z_{10}^m:ten} z_{10}^{\mathrm{m}}[\mathrm{TEN}^*] - (k^-_{z_{10}^m:ten} + k^{\mathrm{cat}}_{z_{10}^m:ten})[Z_{10}^{\mathrm{m}}{:}\mathrm{TEN}^*]. \tag{A.31}$$

A.2.3 *Fluid phase*

$$\frac{\partial z_2}{\partial t} = -\nabla\cdot(\mathbf{u}z_2 - D\nabla z_2) - k_2^{\mathrm{on}} z_2(N_2^{\mathrm{b}} P^{\mathrm{b,a}} + N_2^{\mathrm{se}} P^{\mathrm{se,a}} - z_2^{\mathrm{mtot}} - e_2^{\mathrm{mtot}}) + k_2^{\mathrm{off}} z_2^{\mathrm{m}}, \tag{A.32}$$

$$\begin{aligned}\frac{\partial e_2}{\partial t} = {}& -\nabla\cdot(\mathbf{u}e_2 - D\nabla e_2) - k_2^{\mathrm{on}} e_2(N_2^{\mathrm{b}} P^{\mathrm{b,a}} + N_2^{\mathrm{se}} P^{\mathrm{se,a}} - z_2^{\mathrm{mtot}} - e_2^{\mathrm{mtot}}) + k_2^{\mathrm{off}} e_2^{\mathrm{m}} \\ & + (k^{\mathrm{cat}}_{z_5:e_2} + k^-_{z_5:e_2})[Z_5{:}E_2] - k^+_{z_5:e_2} z_5 e_2 + (k^-_{z_7:e_2} + k^{\mathrm{cat}}_{z_7:e_2})[Z_7{:}E_2] - k^+_{z_7:e_2} z_7 e_2 \\ & + (k^{\mathrm{cat}}_{z_8:e_2} + k^-_{z_8:e_2})[Z_8{:}E_2] - k^+_{z_8:e_2} z_8 e_2 - k_2^{\mathrm{in}} e_2,\end{aligned} \tag{A.33}$$

$$\begin{aligned}\frac{\partial z_5}{\partial t} = {}& -\nabla\cdot(\mathbf{u}z_5 - D\nabla z_5) - k_5^{\mathrm{on}} z_5(N_5^{\mathrm{b}} P^{\mathrm{b,a}} + N_5^{\mathrm{se}} P^{\mathrm{se,a}} - z_5^{\mathrm{mtot}} - e_5^{\mathrm{mtot}}) + k_5^{\mathrm{off}} z_5^{\mathrm{m}} \\ & - k^+_{z_5:e_2} z_5 e_2 + k^-_{z_5:e_2}[Z_5{:}E_2] + N_5 \frac{\partial(P^{\mathrm{b,a}} + P^{\mathrm{se,a}})}{\partial t},\end{aligned} \tag{A.34}$$

$$\begin{aligned}\frac{\partial e_5}{\partial t} = {}& -\nabla\cdot(\mathbf{u}e_5 - D\nabla e_5) - k_5^{\mathrm{on}} e_5(N_5^{\mathrm{b}} P^{\mathrm{b,a}} + N_5^{\mathrm{se}} P^{\mathrm{se,a}} - z_5^{\mathrm{mtot}} - e_5^{\mathrm{mtot}}) + k_5^{\mathrm{off}} e_5^{\mathrm{m}} \\ & + k^{\mathrm{cat}}_{z_5:e_2}[Z_5{:}E_2],\end{aligned} \tag{A.35}$$

$$\begin{aligned}\frac{\partial z_7}{\partial t} = {}& -\nabla\cdot(\mathbf{u}z_7 - D\nabla z_7) - k^+_{z_7:e_{10}} z_7 e_{10} + k^-_{z_7:e_{10}}[Z_7{:}E_{10}] + k^-_{z_7:e_2}[Z_7{:}E_2] \\ & - k^+_{z_7:e_2} z_7 e_2,\end{aligned} \tag{A.36}$$

$$\frac{\partial e_7}{\partial t} = -\nabla\cdot(\mathbf{u}e_7 - D\nabla e_7) + k^{\mathrm{cat}}_{z_7:e_{10}}[Z_7{:}E_{10}] + k^{\mathrm{cat}}_{z_7:e_2}[Z_7{:}E_2],$$

$$\begin{aligned}\frac{\partial z_8}{\partial t} = {}& -\nabla\cdot(\mathbf{u}z_8 - D\nabla z_8) - k_8^{\mathrm{on}} z_8(N_8^{\mathrm{b}} P^{\mathrm{b,a}} + N_8^{\mathrm{se}} P^{\mathrm{se,a}} - z_8^{\mathrm{mtot}} - e_8^{\mathrm{mtot}}) + k_8^{\mathrm{off}} z_8^{\mathrm{m}} \\ & - k^+_{z_8:e_2} z_8 e_2 + k^-_{z_8:e_2}[Z_8{:}E_2],\end{aligned} \tag{A.37}$$

$$\begin{aligned}\frac{\partial e_8}{\partial t} = {}& -\nabla\cdot(\mathbf{u}e_8 - D\nabla e_8) - k_8^{\mathrm{on}} e_8(N_8^{\mathrm{b}} P^{\mathrm{b,a}} + N_8^{\mathrm{se}} P^{\mathrm{se,a}} - z_8^{\mathrm{mtot}} - e_8^{\mathrm{mtot}}) + k_8^{\mathrm{off}} e_8^{\mathrm{m}} \\ & + k^{\mathrm{cat}}_{z_8:e_2}[Z_8{:}E_2],\end{aligned} \tag{A.38}$$

$$\frac{\partial z_9}{\partial t} = -\nabla\cdot(\mathbf{u}z_9 - D\nabla z_9) - k_9^{\mathrm{on}} z_9(N_9^{\mathrm{b}} P^{\mathrm{b,a}} + N_9^{\mathrm{se}} P^{\mathrm{se,a}} - z_9^{\mathrm{mtot}} - e_9^{\mathrm{mtot}}) + k_9^{\mathrm{off}} z_9^{\mathrm{m}}, \tag{A.39}$$

$$\frac{\partial e_9}{\partial t} = -\nabla\cdot(\mathbf{u}e_9 - D\nabla e_9) - k_9^{\mathrm{on}} e_9 (N_9^{\mathrm{b}} P^{\mathrm{b,a}} + N_9^{\mathrm{se}} P^{\mathrm{se,a}} - z_9^{\mathrm{mtot}} - e_9^{\mathrm{mtot}}) + k_9^{\mathrm{off}} e_9^{\mathrm{m}} \tag{A.40}$$

$$- k_9^{\mathrm{in}} e_9 - k_9^{\mathrm{on}} e_9^{\mathrm{m}} (N_{9*}^{\mathrm{b}} P^{\mathrm{b,a}} + N_{9*}^{\mathrm{se}} P^{\mathrm{se,a}} - e_9^{\mathrm{m},*} - [\mathrm{TEN}^*] - [Z_{10}^{\mathrm{m}}{:}\mathrm{TEN}^*])$$

$$+ k_9^{\mathrm{off}} e_9^{\mathrm{m},*},$$

$$\frac{\partial z_{10}}{\partial t} = -\nabla\cdot(\mathbf{u}z_{10} - D\nabla z_{10})$$

$$- k_{10}^{\mathrm{on}} z_{10} (N_{10}^{\mathrm{b}} P^{\mathrm{b,a}} + N_{10}^{\mathrm{se}} P^{\mathrm{se,a}} - e_{10}^{\mathrm{mtot}} - z_{10}^{\mathrm{mtot}}) + k_{10}^{\mathrm{off}} z_{10}^{\mathrm{m}}, \tag{A.41}$$

$$\frac{\partial e_{10}}{\partial t} = -\nabla\cdot(\mathbf{u}e_{10} - D\nabla e_{10})$$

$$- k_{10}^{\mathrm{on}} e_{10} (N_{10}^{\mathrm{b}} P^{\mathrm{b,a}} + N_{10}^{\mathrm{se}} P^{\mathrm{se,a}} - e_{10}^{\mathrm{mtot}} - z_{10}^{\mathrm{mtot}})$$

$$+ k_{10}^{\mathrm{off}} e_{10}^{\mathrm{m}} - k^{+}_{tfpia:e_{10}} [\mathrm{TFPI}] e_{10} + k^{-}_{tfpia:e_{10}} [\mathrm{TFPIa}]$$

$$+ (k^{-}_{z_7:e_{10}} + k^{\mathrm{cat}}_{z_7:e_{10}})[Z_7{:}E_{10}] - k^{+}_{z_7:e_{10}} z_7 e_{10} - k_{10}^{\mathrm{in}} e_{10}, \tag{A.42}$$

$$\frac{\partial [Z_5{:}E_2]}{\partial t} = -\nabla\cdot(\mathbf{u}[Z_5{:}E_2] - D\nabla[Z_5{:}E_2]) + k^{+}_{z_5:e_2} z_5 e_2$$

$$- (k^{-}_{z_5:e_2} + k^{\mathrm{cat}}_{z_5:e_2})[Z_5{:}E_2], \tag{A.43}$$

$$\frac{\partial [Z_7{:}E_2]}{\partial t} = -\nabla\cdot(\mathbf{u}[Z_7{:}E_2] - D\nabla[Z_7{:}E_2]) + k^{+}_{z_7:e_2} z_7 e_2$$

$$- (k^{-}_{z_7:e_2} + k^{\mathrm{cat}}_{z_7:e_2})[Z_7{:}E_2], \tag{A.44}$$

$$\frac{\partial [Z_7{:}E_{10}]}{\partial t} = -\nabla\cdot(\mathbf{u}[Z_7{:}E_{10}] - D\nabla[Z_7{:}E_{10}]) + k^{+}_{z_7:e_{10}} z_7 e_{10}$$

$$- (k^{-}_{z_7:e_{10}} + k^{\mathrm{cat}}_{z_7:e_{10}})[Z_7{:}E_{10}], \tag{A.45}$$

$$\frac{\partial [Z_8{:}E_2]}{\partial t} = -\nabla\cdot(\mathbf{u}[Z_8{:}E_2] - D\nabla[Z_8{:}E_2]) + k^{+}_{z_8:e_2} z_8 e_2$$

$$- (k^{-}_{z_8:e_2} + k^{\mathrm{cat}}_{z_8:e_2})[Z_8{:}E_2], \tag{A.46}$$

$$\frac{\partial [\mathrm{APC}]}{\partial t} = -\nabla\cdot(\mathbf{u}[\mathrm{APC}] - D\nabla[\mathrm{APC}]) - k^{+}_{apc:e_5^m} [\mathrm{APC}] e_5^{\mathrm{m}}$$

$$+ (k^{-}_{apc:e_5^m} + k^{\mathrm{cat}}_{apc:e_5^m})[\mathrm{APC}{:}E_5^{\mathrm{m}}] - k^{+}_{apc:e_8^m} [\mathrm{APC}] e_8^{\mathrm{m}}$$

$$+ (k^{-}_{apc:e_8^m} + k^{\mathrm{cat}}_{apc:e_8^m})[\mathrm{APC}{:}E_8^{\mathrm{m}}], \tag{A.47}$$

$$\frac{\partial[\mathrm{TFPI}]}{\partial t} = -\nabla\cdot(\mathbf{u}[\mathrm{TFPI}] - D\nabla[\mathrm{TFPI}]) - k^{+}_{tfpia:e_{10}}[\mathrm{TFPI}]\mathrm{e}_{10} + k^{-}_{tfpia:e_{10}}[\mathrm{TFPIa}], \tag{A.48}$$

$$\frac{\partial[\mathrm{TFPIa}]}{\partial t} = -\nabla\cdot(\mathbf{u}[\mathrm{TFPIa}] - D\nabla[\mathrm{TFPIa}]) + k^{+}_{tfpia:e_{10}}[\mathrm{TFPI}]e_{10} - k^{-}_{tfpia:e_{10}}[\mathrm{TFPIa}], \tag{A.49}$$

$$\frac{\partial[\mathrm{ADP}]}{\partial t} = -\mathbf{u}\cdot\nabla[\mathrm{ADP}] + \nabla\cdot(D[\nabla\mathrm{ADP}]) + \sigma_{\mathrm{release}}. \tag{A.50}$$

A.2.4. *Subendothelium boundary conditions*

$$-D\frac{\partial e_2}{\partial y} = -k^{+}_{z_7^{se}:e_2} z_7^{\mathrm{se}} e_2 + (k^{-}_{z_7^{se}:e_2} + k^{\mathrm{cat}}_{z_7^{se}:e_2})[Z_7^{\mathrm{se}}{:}E_2], \tag{A.51}$$

$$-D\frac{\partial z_7}{\partial y} = -k_7^{\mathrm{on}} z_7([\mathrm{TF}] - z_7^{\mathrm{se,tot}} - e_7^{\mathrm{se,tot}}) + k_7^{\mathrm{off}} z_7^{\mathrm{se}}, \tag{A.52}$$

$$-D\frac{\partial e_7}{\partial y} = -k_7^{\mathrm{on}} e_7([\mathrm{TF}] - z_7^{\mathrm{se,tot}} - e_7^{\mathrm{se,tot}}) + k_7^{\mathrm{off}} e_7^{\mathrm{se}}, \tag{A.53}$$

$$-D\frac{\partial z_9}{\partial y} = -k^{+}_{z_9:e_7^{se}} z_9 e_7^{\mathrm{se}} + k^{-}_{z_9:e_7^{se}}[Z_9{:}E_7^{\mathrm{se}}], \tag{A.54}$$

$$-D\frac{\partial e_9}{\partial y} = k^{\mathrm{cat}}_{z_9:e_7^{se}}[Z_9{:}E_7^{\mathrm{se}}], \tag{A.55}$$

$$-D\frac{\partial z_{10}}{\partial y} = -k^{+}_{z_{10}:e_7^{se}} z_{10} e_7^{\mathrm{se}} + k^{-}_{z_{10}:e_7^{se}}[Z_{10}{:}E_7^{\mathrm{se}}], \tag{A.56}$$

$$-D\frac{\partial e_{10}}{\partial y} = -k^{+}_{z_7^{se}:e_{10}} e_{10} z_7^{\mathrm{se}} + k^{\mathrm{cat}}_{z_{10}:e_7^{se}}[Z_{10}{:}E_7^{\mathrm{se}}] + (k^{-}_{z_7^{se}:e_{10}} + k^{\mathrm{cat}}_{z_7^{se}:e_{10}})[Z_7^{\mathrm{se}}{:}E_{10}], \tag{A.57}$$

$$-D\frac{\partial[\mathrm{TFPIa}]}{\partial y} = -k^{+}_{tfpia:e_7^{se}}[\mathrm{TFPIa}]e_7^{\mathrm{se}} + k^{-}_{tfpia:e_7^{se}}[\mathrm{TFPIa}{:}E_7^{\mathrm{se}}]. \tag{A.58}$$